Modelling Soil-Transmitted Helminths

Using Generalised Polynomial Chaos

School of Mathematics, Statistics and Computer Science

Siboniso Nqubeko Goba

A thesis submitted to the University of KwaZulu-Natal, College of Agriculture, Engineering and Science, in the fulfillment of the requirements for the degree of Master of Science

Supervisor: Dr. F. Chirove

December 2018

I, Siboniso Nqubeko Goba , declare that:

(i) The research reported in this thesis, except where otherwise indicated, is my original research.

(ii) This thesis has not been submitted for any degree or examination at any other university.

(iii) This thesis does not contain other persons' data, pictures, graphs or other information, unless specifically acknowledged as being sourced from other persons.

(iv) This thesis does not contain other persons' writing, unless specifically acknowledged as being sourced from other researchers. Where other written sources have been quoted, then:

a) their words have been re-written but the general information attributed to them has been referenced:

b) where their exact words have been used, their writing has been placed inside quotation marks, and referenced.

(v) This thesis does not contain text, graphics or tables copied and pasted from the Internet, unless specifically acknowledged, and the source being detailed in the dissertation/thesis and in the References sections.

Candidate: Siboniso Nqubeko Goba

Signature: _____

As the candidate's supervisor I agree to the submission of this thesis for examination.

Supervisor: Dr. F. Chirove

Signature: _____

ABSTRACT

Modelling Soil-Transmitted Helminths Using Generalised Polynomial Chaos

Siboniso Nqubeko Goba
School of Mathematics, Statistics and Computer Science
Master of Science

Soil-transmitted helminths are the group of neglected tropical diseases for humans caused by parasitic worms; *Ascaris lumbricoides, Trichuris trichiura* and hookworm species. It occurs mostly in tropical and subtropical regions as it survives in warm and moist temperature. The disease is a severe public health problem as it is prevalent to school-aged children. In this study, a non-linear mathematical model is formulated to model the transmission dynamics and the spread of soil-transmitted Helminths. Firstly, the deterministic model is formulated, and the stability analysis of the model was performed. The disease-free equilibrium is globally asymptotically stable for the basic reproduction number $R_0 < 1$, while for $R_0 > 1$, a unique endemic equilibrium exists and is globally asymptotically stable. Secondly, we apply the polynomial chaos approach to the system of differential equations with random coefficients. This approach takes into account the randomness in the model parameters. The polynomial chaos is applied resulting in a system of coupled ordinary differential equations. The resulting system is solved numerically to obtain the first-order and second-order moments of the stochastic output processes. Sensitivity analysis based on Sobol indices is also employed to determine parameters with the most significant influence on the output. Finally, both deterministic and polynomial chaos simulations reveal that the reduction of the contact rate can reduce the size of the epidemic. The polynomial chaos numerical simulations show low volatility in the number of susceptibe, exposed and infectious human population compared to the egg and larva density which is chaotic.

Keywords: *ascaris lumbricoides, trichuris trichiura*, hookwork, polynomial chaos

ACKNOWLEDGMENTS

I would first like to thank my thesis advisor Dr F Chirove. The door to Dr Chirove's office was always open whenever I ran into trouble or had a question about my research and writing. He constantly allowed this paper to be part of my work, but steered me in the right direction whenever he thought I needed it.

I would also like to express my profound gratitude to my parents, Mr Sipho Goba and Mrs Rebecca Goba for providing with unfailing support and continuous encouragement throughout my years of study and throughout the process of researching and writing this thesis. This accomplishment would not be possible without them. Thank you.

Contents

List of Figures

List of Tables

Chapter 1

Introduction

1.1 Background Of Soil Transmitted Helminths

Soil-transmitted helminthiases (STH) are the group of neglected tropical diseases (NTD) for humans caused by parasitic worms; *ascaris lumbricoides, trichuris trichiura* and hookworm species. The human population get infected through contact with the parasite's egg or larva in the soil. For *ascaris lumbricoides* and *trichuris trichiura* a fully developed egg is ingested for the infection to occur. Ingestion can happen in many ways such as consumption of vegetables which are not carefully washed or cooked [10]. Hookworm larva penetrates the skin of the host for infection, and this usually happens when people are walking barefoot [10]. Inside the host, developed hookworm stay in the upper part of the human small intestine, whereas *ascaris lumbricoides* stay in the entire small intestine and *trichuris trichiura* stay in the large intestine [8]. The worms feed on intestinal host tissues including blood, which result in the loss of iron and protein [10, 11]. The worm burden is prevalent in the tropical and subtropical region as it survives in warm and moist temperature [11, 12]. Light infection in most cases has no symptoms. However, heavier worm presence causes more symptoms such as malnutrition, malabsorption, abdominal pain, cramping and tiredness, and

impaired cognitive and physical development [13].

In 2010 the global STH infection estimate was 43.9 million, 819.0 million and 464.6 million people for Hookworm, *ascaris* and *truchuris* respectively [14], which means more than 1.3 billion people in the world are infected with STH [14]. An estimate of 568 million school-age children (SAC) in the world live in areas endemic to STH. The worldwide prevalence estimate of STH is more than that of HIV/AIDS, tuberculosis and malaria [15]. More infections recorded are from pre-SAC and SAC sub-populations living in poor and malnourished communities. The world health organisation (WHO) in 2016 estimated that more than 3 million Pre-SAC population in South Africa required treatment for STH and more than 2 million SAC population also need the treatment. WHO recommended that endemic countries should control disease morbidity through periodic treatment of at-risk people. In endemic areas treatment should be given once a year when the baseline prevalence of soil-transmitted helminth infections is over 20% and twice a year when the prevalence of soil-transmitted helminth infections is over 50% [10]. Most studies revealed that inadequate hygiene, poor health care systems and facilities, social instability, civil war, and natural disasters make the situation worse [16, 17].

1.2 Soil-Transmitted Helminths Life Cycle.

Soil-transmitted helminths worm species have different life cycles. In this section, we discuss the life cycles for three worm species affecting humans, namely *ascaris lumbricoides*, *trichuris trichiura* and hookworm.

1.2.1 *Ascaris lumbricoides*

Adult *ascaris* worms stay in the small intestine of the human host. A female adult worm release about 200 000 eggs per day through the human stool. They release both fertile and infertile (which are not infective) eggs. Fertilised eggs embryonates and become infective after about 18 days depending on environmental conditions. Infective eggs are then ingested and hatch into larvae which invades intestinal mucosa and carried into the lungs via the blood [18]. In the lungs, the larva breaks into the alveoli and pass up the trachea, where they are coughed up and may be swallowed [18]. Upon reaching the small intestines they develop into adult worms. The cycle takes 2 to 3 months. The adult worms in the intestine can live for about 1 to 2 years. Figure 1.1 show the full cycle for *ascaris* worm development [8].

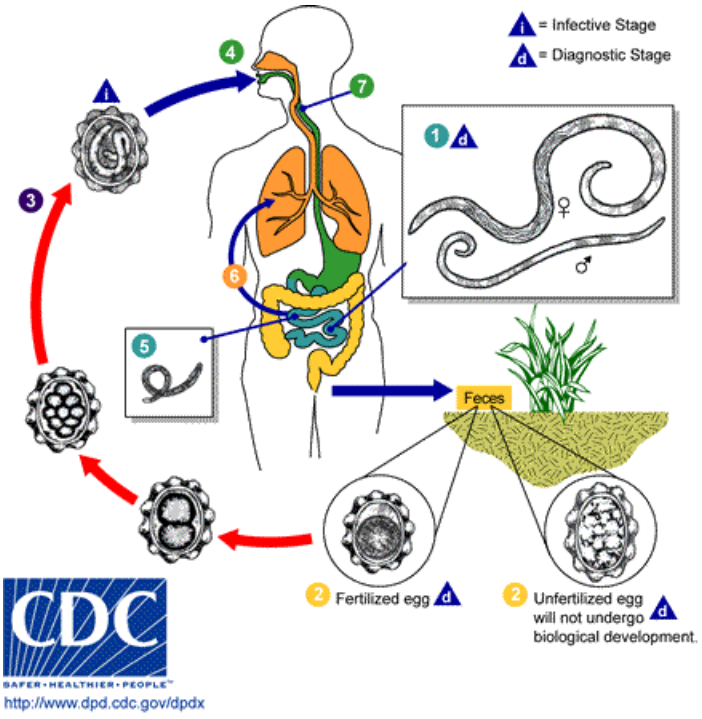

Figure 1.1 Life cycle of *ascaris lumbricoides*. Source [8].

1.2.2 *Trichuris trichiura*

Trichuris egg is deposited into the soil before embryonation. In the soil it undergoes embryonation in two stages; 2-cell stage and advanced cleavage which takes up to 15 to 30 days. Once the egg have embryonated it becomes infective. Human hosts then ingest infective eggs for infection to occur. After ingestion, the egg hatch in the small intestine and become a larva. The larva grow and establish itself as the adult worm in the colon. Adult female larva start to shed eggs into the environment after 60 to 70 days of initial infection. Approximately 3000 to 20000 eggs per day are realised by adult female worms. The adult worms in the colon have the lifespan of up to one year. Figure 1.2 show the diagrammatic representation of this process [8].

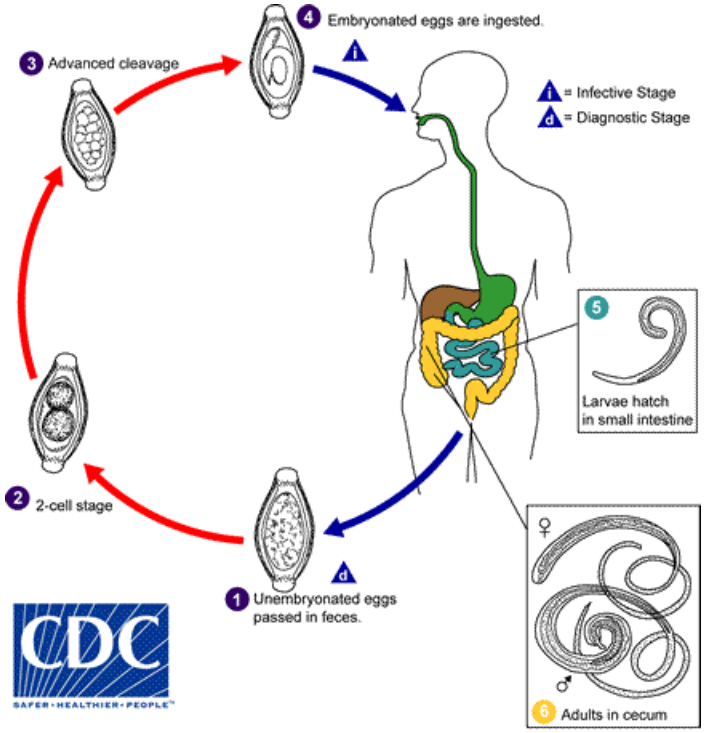

Figure 1.2 Life cycle of *trichuris trichiura*. Source [8].

1.2.3 Hookworm

Hookworm egg is passed in the stool of heavily infected individuals into the soil. In about 1 to 2 days, the egg hatch into first stage larva called *rhabditiform* if environmental conditions (warmth and moisture) are conducive. The first stage larva grows in the soil and becomes *filariform* larva. *Filariform* larva is infective and can survive in the soil for about 3 to 5 weeks. Upon interaction of *filariform* larva with human, they penetrate the skin and move through the blood vessels to the heart and then to the lungs. They gain entrance to the pulmonary alveoli and invade the bronchial tree to the pharynx before being swallowed to the small intestine. The adult worms in the lumen of the small intestine feed on blood tissues, which may result in blood loss of the host. Adult worms stay in the small intestine for 1 to 2 or several years. Figure 1.3 shows the diagrammatic representation of the life cycle for Hookworm in humans [8].

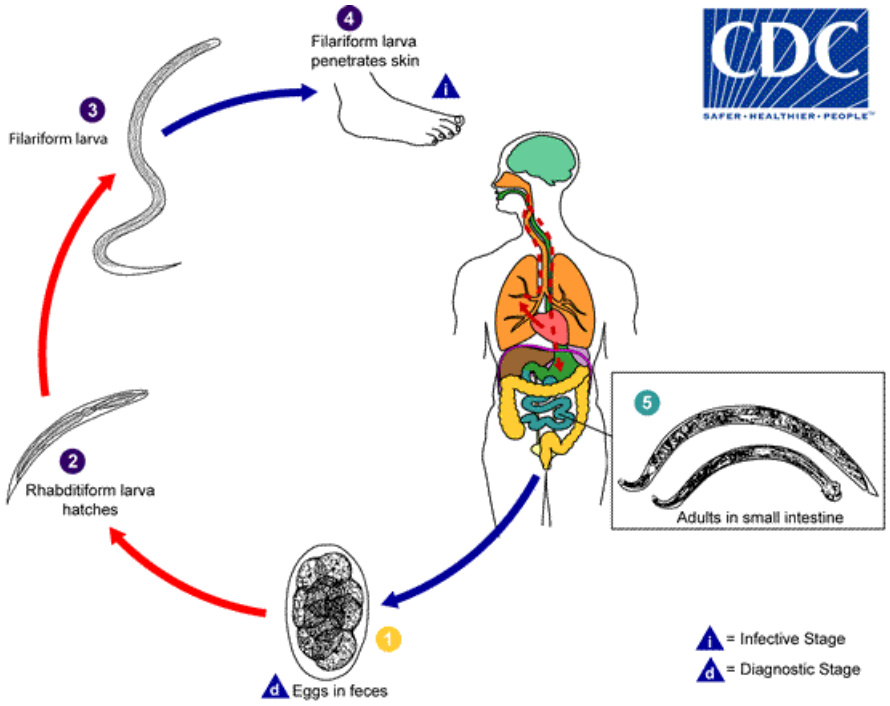

Figure 1.3 Life cycle of hookworm species. Source [8].

1.3 Diagnosis

Infection detection is achieved by stool examination for the presence of STH species eggs. The most common procedure in population studies is the Kato-Katz method. This method is based on faecal smear and microscopy examination, it is also recommended by WHO as the method of STH infection detection. However, the sensitivity of detection for Kato-Katz is low, especially for light intensity infections. Some studies have also revealed that multi stool examination reduces the diagnostic error, hence getting accurate prevalence estimate [19].

1.4 Problem Statement

Despite preventative chemotherapy treatment STH remains the public health problem in poor Asian, American and sub-Saharan Africa with more than 2 billion people infected in more than 100 countries worldwide [20]. More than 267 million pre-SAC and more than 568 million SAC stay in areas where the transmission of these parasites is intense, and are in need of treatment and preventive interventions [20]. Little change has been observed in the prevalence of STH in sub-Saharan Africa, more than one billion people are still infected [21]. In a study conducted in 15 schools in rural South Africa, almost all the schools required treatment for STH infection once or twice a year according to WHO guidelines [22]. In studies conducted in some areas of Kwa-Zulu Natal and Western Cape, the prevalence of STH was more than 50% as shown on the map in Figure 1.4 [9]. Strategies such as preventative chemotherapy have been employed in communities and villages at risk in the attempt to eradicate the disease. There is still more work needed to improve sanitation in endemic areas. Unlike most tropical diseases, very minimal research work on mathematical models in population level for STH is available in the literature [23]. In this work, the STH population model is formulated. The model is designed to study dynamics at the population level. Deterministic and stochastic method using generalized polynomial chaos is employed in

the analysis of the model. Bio-mathematical models are useful for government and public health practitioners to help in formulating policies and proper plan for treatment administration based on the processes and patterns of the interacting species.

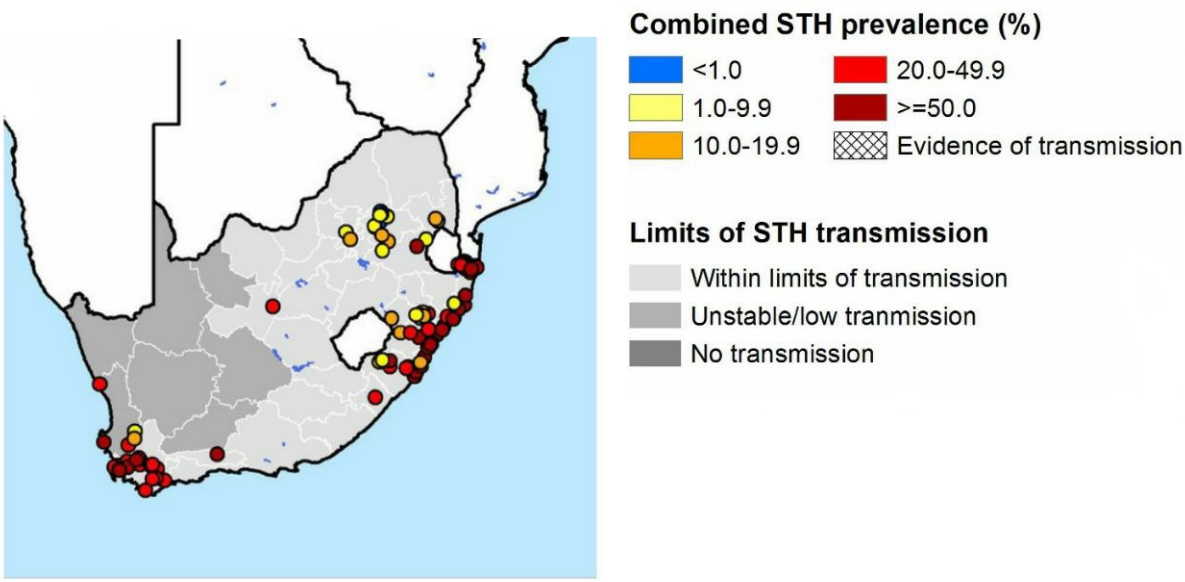

Figure 1.4 South African distribution of soil-transmitted helminths. Source [9]

.

1.5 Aim and Objectives

1.5.1 Aim

The aim of this project is to quantify uncertainty in the model parameters for the soil-transmitted helminths using generalised polynomial chaos.

1.5.2 Objectives

1. To develop and analyse a population model to capture soil-transmitted helminths dynamics.

2. To apply generalised polynomial chaos in the model to capture parameters uncertainty.

1.6 Generalised Polynomial Chaos Preliminaries

1.6.1 Orthogonality of polynomials

Definition 1. *[24] Let U be the interval in $\mathbb{R}$. A **weight function** $\xi(x)$ is a nonnegative integrable function of $x \in U$.*

Definition 2. *[24] For any functions $f, g \in L_\xi(U)$, the **inner product** of f and g is*

$$\langle f, g \rangle = \int_U f(x)g(x)\xi(x)dx \tag{1.1}$$

Definition 3. *[25] A **Hilbert space** is a vector space L_ξ with an inner product $\langle f, g \rangle$ such that the norm defined by $|f| = \sqrt{(}\langle f, f \rangle)$ turns L_ξ into a complete metric space.*

Definition 4. *[24] Let U be an interval in $\mathbb{R}$. Let f and g be two functions in a Hilbert space $L_\xi(U)$. The functions f and g are **orthogonal functions** if*

$$\langle f, g \rangle = 0 \tag{1.2}$$

Definition 5. *[24] The function P_n is a **polynomial** of degree n if there is a sequence of real numbers $\alpha_i \in \mathbb{R}$ for $i = 1, 2, 3, \ldots, n$ such that*

$$P_n(x) = \sum_{i=0}^{n} \alpha_i x^i \tag{1.3}$$

where $x \in U$

Definition 6. *[24] The set of polynomials $\{P_n^+\}$ are **orthogonal polynomials** if P_n^+ is a polynomial of degree n and:*

$$\langle P_i^+, P_j^+ \rangle = 0, \quad for \quad i \neq j \tag{1.4}$$

We assume that for all orthogonal polynomials of degree zero

$$P_0^+(x) = 1, \quad x \in U \tag{1.5}$$

Theorem 1. *[24] Let $\{P_n^+\}$ be a set of orthogonal polynomials and $\xi(x)$ be weight function. The integral*

$$\int_U P_0^+(x)\xi(x)dx = \int_U \xi(x)dx \tag{1.6}$$

Moreover, for $n \geq 1$ we have

$$\int_U P_n^+(x)\xi(x)dx = 0 \tag{1.7}$$

Proof. From (1.5) proving (1.6) is easy. For the case of $n \geq 1$

$$\begin{aligned}\int_U P_n^+(x)\xi(x)dx &= \int_U P_0^+(x)P_n^+(x)\xi(x)dx \\ &= \langle P_0^+(x), P_n^+(x)\rangle \\ &= 0\end{aligned}$$

by definitions 2 and 6. □

Theorem 2. *[24] For U an interval in $\mathbb{R}$ and ξ a weight function in U, the function*

$$f(x) = \frac{\xi(x)}{\int_U \xi(x)dx}$$

for $x \in U$ is a probability density function.

Proof. The proof is straight forward,

$$\begin{aligned}\int_U f(x)dx &= \int_U \frac{\xi(x)dx}{\int_U \xi(x)dx} \\ &= \frac{1}{\int_U \xi(x)dx}\int_U \xi(x)dx \\ &= 1\end{aligned}$$

□

Theorem 3. *[24] Let $\{P_n^+\}$ be a set of orthogonal polynomials. Assume that x is a random variable associated with the probability density function f, from weight function ξ. The expected value of $P_n(x)$ is given by*

$$E(P_n(x)) = \begin{cases} 1, & for \quad n = 0 \\ 0. & for \quad n \geq 1 \end{cases} \tag{1.8}$$

and the variance is given by:

$$V(P_n^+(x)) = \begin{cases} 0, & for \quad n = 0 \\ \frac{\langle P_n^+, P_n^+ \rangle}{\int_U \xi(x)dx}, & for \quad n \geq 1 \end{cases}$$

Proof. For $n = 0$, by definition of expectation we have:

$$\begin{aligned} E(P_0^+(x)) &= \int_U P_0^+(x) f(x) dx \\ &= \int_U f(x) dx \\ &= 1, \end{aligned}$$

since $P_0^+(x)$ is the constant, $V(P_0^+(x)) = 0$.

For $n \geq 1$,

$$\begin{aligned} E(P_n^+(x)) &= \int_U P_n^+(x) f(x) dx \\ &= \int_U P_n^+(x) \frac{\xi(x)}{\int_U \xi(x)dx} \\ &= \frac{1}{\int_U \xi(x)dx} \int_U P_n^+(x) \xi(x) dx \\ &= 0, \end{aligned}$$

by Theorems 1 and 2.

Using the definition of variance, we have

$$\begin{aligned} V(P_n^+(x)) &= E[(P_n^+(x) - E(P_n^+(x)))^2] \\ &= E(P_n^+(x)^2) \\ &= \int_U P_n^+(x)^2 f(x)dx \\ &= \frac{1}{\int_U \xi(x)dx} \int_U P_n^+(x)^2 \xi(x)dx \\ &= \frac{\langle P_n^+, P_n^+ \rangle}{\int_U \xi(x)dx} \end{aligned}$$

from definition 2 and Theorem 2. □

1.6.2 Generalized Polynomial Chaos.

The idea of polynomial chaos was first introduced by Wiener [26], in a problem involving independent Gaussian random variables. The Hermite polynomial was used as a basis function. Xiu and Karniadakis [27] expanded the idea to generalised polynomial chaos (GPC). They noticed that Hermite polynomials can be used in solving stochastic differential equations (SDE) involving random variables. Generalized polynomial chaos is a way of representing stochastic processes parametrically using a set of random variables. For example, consider the probability space $(\Omega, \mathscr{A}, \mathscr{P})$, where Ω is the event space, $\mathscr{A} \in 2^\Omega$ is an σ-algebra and $\mathscr{P}$ its probability measure. A stochastic process $X(\omega)$ governed by a set of random variables $\{\zeta_1(\omega), \zeta_2(\omega), \zeta_3(\omega) \ldots, \zeta_N(\omega)\}$ is given by

$$X(\omega) = \sum_{i=0}^{\infty} \alpha_i \Psi_k(\zeta(\omega)), \tag{1.9}$$

where $\omega \in \Omega$ is the event and $\{\Psi_k(\zeta(\omega)\}$ is a set of orthogonal polynomials. Each probability distribution function is assigned to a family of orthogonal polynomials as shown in Table 1.1. The expansion given by equation (1.9) can be truncated by reducing the expansion to finite-dimension and set the significant highest order of polynomial $\{\Psi\}$. The stochastic process in the N-dimension

Distribution	Random variable	Polynomial	Support
Continuous	Gaussian	Hermite	$(-\infty,\infty)$
	Gamma	Lauegerre	$[0,\infty]$
	Beta	Jacobi	$[a,b]$
	Uniform	Legendre	[a,b]
Discrete	Poisson	Charlier	$\{0,1,2,\dots\}$
	Binomial	Krawtchouk	$\{0,1,2,\dots,N\}$
	Negative binomial	Meixner	$\{0,1,2,\dots\}$
	Hyper geometric	Hahn	$\{0,1,2,\dots,N\}$

Table 1.1 Distribution functions with their corresponding orthogonal polynomials

form is given by

$$X(\omega) = \sum_{i=0}^{M} \alpha_i \Psi_k(\zeta(\omega)), \tag{1.10}$$

where $\zeta = (\zeta_1, \zeta_2, \dots, \zeta_N)^T$ is N-dimensional random vector. Let us denote the highest order of the polynomial by P, then the total number of expansions $M+1$ is calculated as

$$M+1 = \frac{(N+1)!}{N!P!} \tag{1.11}$$

1.6.3 General Stochastic Garlerkin Algorithm [1]

Let us consider the stochastic differential equation

$$\mathscr{L}(\mathbf{Y},t,\omega;X) = f(\mathbf{Y},t;\omega), \tag{1.12}$$

where $X =: X(\mathbf{y},t;\theta)$ is the solution and $f(\mathbf{Y},t;\omega)$ is the source function. The operator $\mathscr{L}$ generally involves differentiation in space/time and it can be nonlinear. Boundary conditions and initial conditions are assumed. The random parameter ω exists because of the introduction of uncertainty

into the system. Uncertainty can be introduced in the system through boundary conditions, initial conditions, material properties, etc. The solution, X, is regarded as the random process and can be expanded by the truncated Wiener-Askey polynomial chaos defined by equation (1.10).

Next, we substitute equation (1.10) into the differential equation

$$\mathscr{L}\left(\mathbf{Y},t,\omega;\sum_{i=0}^{M}\alpha_i\Psi_k(\zeta(\omega))\right)=f(\mathbf{Y},t,\omega) \tag{1.13}$$

The choice of ξ and $\{\Psi_k\}$ defines a weight function for an inner product. Using this inner product, we take a Galerkin projection of the differential equation onto each basis polynomial Ψ_i.

$$\left\langle \mathscr{L}\left(\mathbf{Y},t,\omega;\sum_{i=0}^{M}\alpha_i\Psi_k(\zeta(\omega))\right),\Psi_i\right\rangle=\langle f(\mathbf{Y},t,\omega),\Psi_i\rangle \tag{1.14}$$

The projection ensures that the error in the approximate solution is orthogonal to the space spanned by $\{\Psi_k\}$. By the orthogonality of $\{\Psi_k\}$, the stochastic differential equation reduces to a system of coupled deterministic differential equations for the coefficients of the truncated PCE. We can use any appropriate spatial and temporal discretization of the coefficients to solve this system.

1.7 Mathematical Modelling Tools

Let consider the dynamical system

$$\dot{x}(t)=f(t,x),\quad x\in\mathbb{R}^n \tag{1.15}$$

1.7.1 The Equilibrium Point And Its Stability [2]

Definition 7. *$X^*\in\mathbb{R}^n$ is said to be an equilibrium point of equation (1.15) if $f(t,X^*)=0$ for all t.*

Definition 8. *An equilibrium point X^* of the system in (1.15) is said to be*

1. ***Stable*** *if for any positive scalar* δ *there exist a positive scalar* σ *such that* $||X(t_0)|| < \sigma$, $||X(t)|| < \delta$ *for all* $t \geq t_0$.

2. ***Asymptotically stable*** *if it's stable and*

$$\lim_{t\to\infty} X(t) \to X^*$$

3. ***Unstable*** *if is not stable.*

1.7.2 Lyapunov Local Stability Theorem [3]

Consider the map

$$\dot{x}(t) = f(t,x), \quad X_e = 0. \tag{1.16}$$

Define the Lyapunov function V: $\mathscr{N} \to \mathbb{R}$ as a function which satisfies the following properties:

1. $V(x)$ and its partial derivatives are continuous.

2. $V(x)$ is positive definite.

3. $\dot{V}(x)$ is negative semidefinite.

Theorem 4. *If there exists a Lyapunov function for the system of equation (1.16), then* $X_e = 0$ *is stable.*

Theorem 5. *(**Lyapunov direct method**). If there exists a Lyapunov function for the system of equation (1.16), with the additional propery that* $\dot{V}(x)$ *is negative definite then* $X_e = 0$ *is asymptotically stable.*

Theorem 6. *If there exists a positive definite function V for which* $\dot{V}(x)$ *is also positive definite for the system of equation (1.16), then* $X_e = 0$ *is unstable.*

1.7.3 Lyapunov Direct Global Stability Theorem [3]

The theorems for Lyapunov global stability are similar with the local stability theorems, except for the following differences

1. $\mathscr{N} \to \mathbb{R}^n$ and
2. $V(x) \to \infty$ as $||X|| \to \infty$. A function with this property is said to be radially unbounded and its needed to ensure that the contours of V define closed curves.

1.7.4 Lyapunov Indirect Local Stability [4]

Let us define the system of differential equations

$$\frac{dx}{dt} = f(x), \tag{1.17}$$

where $f : \mathrm{D} \to \mathbb{R}^n$ is continuously differentiable and D is close to x^*. Let X^* be an equilibrium point of the system of differential equations (1.17). The Jacobian matrix of equation (1.17) evaluated at the equilibrium point x^* is given by

$$M = \left.\frac{\partial f}{dx}\right|_{X=X^*}.$$

The linearised system of (1.17) is given by

$$\frac{du}{dt} = Mu, \quad u = x - x^* \tag{1.18}$$

then

1. x^* is asymptotically stable if $\mathrm{Re}(\lambda_i(A)) < 0$ for $i = 1, \ldots, n$.
2. x^* is unstable if $\mathrm{Re}(\lambda_i(A)) > 0$ for at least one i.

$\mathrm{Re}(\lambda_i(A))$ is the real part of the i^{th} eigenvalues of A. Stability defined by indirect method is called local stability because A is only defined at x^*, hence the stability is restricted to the small neighborhood of x^*.

1.7.5 Centre Manifold Theorem [5]

Theorem 7. *Let consider the ordinary differential equation:*

$$\frac{dx}{dt} = f(x,\phi), \quad f : \mathbb{R}^n \times \mathbb{R} \to \mathbb{R} \quad \text{and} \quad f \in \mathbb{C}^2(\mathbb{R}^n \times \mathbb{R}) \tag{1.19}$$

Let assume 0 *is an equilibrium point for the system for values of the parameter* ϕ*, that is :*

$$f(0,\phi) = 0, \quad \text{for all} \quad \phi$$

Let assume

- $A = D_x f(0,0) = \left(\frac{\partial f_i}{\partial x_j}(0,0)\right)$ *is the linearisation matrix of the system around the equilibrium point* 0 *with the parameter* ϕ *evaluated at* 0*. In simple terms, zero is the eigenvalue of A and all other eigenvalues of A have negative real parts.*

- *Matrix A has nonnegative right eigenvector v and a left eigenvector w corresponding to the zero eigenvalue.*

Lets assume f_k *to be the* k^{th} *element of* f *and*

$$a = \sum_{k,i,j=1}^{n} w_k v_i v_j \frac{\partial^2 f_k}{\partial x_i \partial x_j}(0,0),$$
$$b = \sum_{k,i=1}^{n} w_k v_i \frac{\partial^2 f_k}{\partial x_i \partial \phi}(0,0).$$

The local dynamics of equation (1.19) are determined by a and b as follows:

1. $a > 0, b > 0$*. When* $\phi < 0$ *with* $|\phi| << 0$ *is locally asymptotically stable, and there exists a positive unstable equilibrium;* $0 < \phi << 1$ *is unstable and there exists a negative and locally asymptotically stable e quilibrium;*

2. $a < 0, b < 0$*. When* $\phi < 0$ *with* $|\phi| \ll 0$ *is unstable; when* $0 < \phi \ll 1$*, 0 is locally asymptotically stable, and there exists a positive unstable equilibrium;*

3. *$a > 0, b < 0$. When $\phi < 0$ with $|\phi| \ll 0$ is unstable, and there exists a locally asymptotically stable negative equilibrium; when $0 < \phi \ll 1$, 0 is stable, and a positive unstable equilibrium appears;*

4. *$a < 0, b > 0$. When ϕ changes from negative to positive, 0 changes its stability from stable to unstable. Correspondingly a negative unstable equilibrium becomes positive and locally asymptotically stable.*

1.7.6 The Basic Reproduction Number [6]

In the study of epidemics, the basic reproduction number measures the expected number of secondary infections that may result if one infectious individual is introduced in the purely susceptible population. One method used to calculate this quantity is the next generation matrix. This section discusses this method briefly.

Let $\mathbf{x} = (x_1, x_2, \ldots, x_n)^T$ represent the size of each compartment, where the first $m < n$ compartments contain infected individuals. Assume that the disease free equilibrium $\mathbf{x}_0$ exists and it is stable. Consider the system of differential equations for $x_1, x_2, \ldots, x_n$ written in the form

$$\frac{dx_i}{dt} = \mathscr{F}_i(x) - \mathscr{V}_i(x) \quad \text{for} \quad i = 1, 2, \ldots, m$$

where $\mathscr{F}_i(x)$ is the rate of appearance of new infection in compartment i and $\mathscr{V}_i(x)$ is the rate of transition between compartment i and other compartments. Now, let define the matrices

$$F = \left(\frac{\partial \mathscr{F}_i(x_0)}{\partial x_j} \right), \quad V = \left(\frac{\partial \mathscr{V}_i(x_0)}{\partial x_j} \right) \quad \text{for} \quad 1 \leq i, j \leq m$$

The next generation matrix is given by FV^{-1}. The basic reproduction number is calculated as the spectral radius of FV^{-1} and it is given by

$$R_0 = \rho(FV^{-1}).$$

1.7.7 The Descartes Rule Of Signs [7]

The Descartes rule of signs is a method used to examine signs of a polynomial function roots. Let us consider the polynomial

$$P(x) = a_0 + a_1x + a_2x^2 + \cdots + a_nx^n$$

where $a_0, a_1, a_2, \ldots, a_n$ are real constants and $a_n \neq 0$. The polynomial $P(x)$ has n number of roots. The concept of Descartes of finding the signs of these roots is given as follows:

1. The number of positive real roots of $P(x)$ is either equal to the number of sign change in the coefficients of $P(x)$ or less than this by an even number.

2. The number of positive real roots of $P(-x)$ is either equal to the number of sign change in the coefficients of $P(-x)$ or less than this by an even number.

1.7.8 The Expected value(Mean) [28]

Definition 9. *Let $f(x)$ be the probability density function of the random variable X in the space S and the summation*

$$\sum_{x \in S} u(x)f(x) \tag{1.20}$$

exists, then the sum is called the mathematical expectation or expected value of $u(x)$ and is denoted by $E(u(x))$. That is

$$E(u(x)) = \sum_{x \in S} u(x)f(x) \tag{1.21}$$

Theorem 8. *If the mathematical expectation, E exists, it satisfies the following properties if a, b are constant and u, v are function:*

1. $E(a) = a$

2. $E(au(x)) = aE(u(x))$

3. *E(au(x)+bv(x))=aE(u(x))+bE(v(x))*

1.8 Thesis outline.

Chapter 2 begins by providing literature review based on mathematical models on soil-transmitted helminths and uncertainty qualification using generalized polynomial chaos. In chapter 3 we formulate the basis deterministic model and analyse its solutions analytically. Transmission parameters uncertainty is included to the model using GPC in chapter 4, which results in the system of coupled ordinary differential equations. Models presented in chapter 3 and 4 are analysed numerically in chapter 5 and we discuss the results. Chapter 6 we conclude our work with relevant recommendations for further research work.

1.9 Summary

This chapter outlined the background information on soil-transmitted helminths infection. We presented different worm species affecting the human population, their life cycles and popular method of disease diagnosis. Statistics in the South African and the whole world context were discussed. The statistics showed why it is important to study soil-transmitted helminths dynamics at the population level. The problem statement, aims and objective of the study were stated in details. We also provided in detail mathematical preliminaries, which will be applied in this study in the later chapters. The significance of the study was also stated, we revealed the contribution this study could make in the public health policy making. Finally, this chapter gave the outline of this study.

Chapter 2

Literature review

2.1 Mathematical models

The earliest work on mathematical models for STH was reviewed by Anderson and May [29]. They looked at the most published models on intestinal nematodes which consist of two equations describing the changes in the densities of adult worms and infective state. The model describing the mean number of sexually mature worms in-host has two loss terms. The gain term represents parasite recruitment to sexually mature worms. The two lost terms in the mean number of worms are worm natural death and host species death. The model also describes dynamics of the infective stage in the environment, this is described by one gain term and two lost terms. This model is developed deterministically but has some probability elements. Among the number of conclusions drawn for their analysis is that the substantial changes in parasite intensity do not result in concomitant changes in the prevalence and also the direct relation of STH infection to worm burden.

Truscott, Hollingworth and Anderson [30] modelled the interruption of transmission of soil-transmitted helminths by repeated mass chemotherapy of school-aged children. They formulated and analysed

the age-structured model of STH population dynamics with regular treatment. The aim of their study was to use models derived from age-structured hybrid to design mass drug administration (MDA) program. They employed an existing model and included dynamics of infectiousness in the environment and worm sexual reproduction. They investigated eradication with finite rounds of treatment and its dependencies in the value of the basic reproduction number and treatment frequencies. They first analysed the stability of a model with no sexual reproduction under treatment. Their analysis revealed that de-worming has a significant impact on worm load and infectiousness in the reservoir in the environment. They also concluded that treatment produces an immediate effect on worm burden, but the population also gets reinfected because of infectious material in the environment. The analysis for model considering sexual reproduction shows that it easier to interrupt transmission in the presence of sexual reproduction term in the model.

A Monstresor [31] analysed the data for soil-transmitted helminths prevalence in the Philippines. They used the Markov chain to develop transitional probability model to predict prevalence changes when only baseline data are available. The model initially assigns each individual to different condition states according to their worm intensity. There are four conditions, state zero, light, moderate and high-intensity egg presence defined by world health organisation. The movement of individuals into different condition state is defined by transition probability. Using the observed baseline prevalence data, the result showed that the model predicted the prevalence change for *Ascaris* better than other STH worm species. The prevalence of hookworms was predicted less precisely than for other STH species. This is probably because hookworms are two different species with different response to anthelminthics, but all the studies they considered did not distinguish, they were all reported as "hookworms".

2.2 Polynomial chaos in differential equations

Chen-Charpentier, Cortes and Romero [32] employed generalized polynomial chaos in the analysis of airy random differential equation. They assumed a different statistical distribution for each random parameter. They expanded each parameter with respect to their generalized polynomial chaos basis function [27]. They explored the representation of solutions as polynomials with different statistical distribution, rather than using Hermite polynomial with parameters assumed to be normally distributed. They also studied the possibility of having random model parameters represented in different basis functions. The study revealed that the choice of the distribution of random model parameters plays an important role in approximating the solution of random differential equations by generalized polynomial chaos, this conclusion was also supported by the gPC-based sobol's indices.

Roberts [33] used generalized polynomial chaos in the epidemic model with uncertainty in the reproduction number. Kermack-McKendrick model was analysed with reproduction number represented as the probability distribution instead of single value. State variables were then expanded in orthogonal polynomials. The reproduction number was varied into three statistical distributions, namely, the beta, normal and uniform distribution. They used H1N1 influenza data for numerical simulations. He concluded that if the range of reproduction number is known the uniform distribution is appropriate and if the estimate is obtained with likelihood profile assumed to be normally distributed, then solutions may be approximated by the beta distribution.

Santonja and Chen-Charpentier [34] applied generalized polynomial chaos in obesity model with uncertainty in model parameters. They considered transmission parameters to be random, the probability distribution. Due to the minimal data points available, the assumed transmission parameters followed the uniform distribution because of its non-informative form. Polynomial

chaos-based Sobol's indices were used for sensitivity analysis. Sensitivity analysis showed that the rate at which people aged between $24-65$ years contribute more to the overall obesity prevalence. They also showed the usefulness of the application of polynomial chaos to an epidemiological model to determine the epidemic evolution close to reality than the deterministic approach.

Minimal studies are available in literature applying generalised polynomial chaos in the epidemic models. Reviewed studies in this section are going to form the building blocks of the current study on helminths infection.

2.3 Summary

In this chapter, we reviewed different papers about mathematical models and data analysis of soil-transmitted helminths. Epidemic models reviewed focuses mostly on the in-host dynamics of the disease with little available literature studying population dynamics. We also reviewed studies on the application of generalised polynomial chaos in the system of differential equations. Most of the studies available in the literature apply this method in engineering uncertainty studies. In our study, we apply this method to the epidemic model.

Chapter 3

Soil-Transmitted Helminths Deterministic Model

This section presents a basic transmission model for soil-transmitted helminths species interacting with the human host population. This model captures the critical stages of the life cycles of the species. We consider three stages of infection in the human population and two stages of the worm development in the soil. We analyse the model by showing that the model is positively invariant and bounded in a feasible region, calculating the reproduction number and determining equilibrium points and their stability.

3.1 Model Formulation

We consider the human host population interacting with STH eggs and larvae in the soil. The human population is stratified into three subpopulations; the susceptible humans; S, which represents individuals who are free of worm burden but at risk of acquiring the infection, the exposed hosts, E, represents individuals who have interacted with the contaminated soil by walking barefoot and get penetrated by the hookworm larva or ingested eggs but they are not shedding eggs in the soil

yet, the infectious hosts, I, represents individuals with fully developed worms in the intestine that produces eggs to be deposited in the soil. The density of eggs in the soil is denoted by W_e and finally, the infectious larva density is represented by W_l. Individuals move from one compartment to another as the worm develops inside the host after infection. The total human population is given by

$$N(t) = S(t) + E(t) + I(t). \tag{3.1}$$

We have assumed that the infection can only occur when individuals interact with contaminated soil through ingestion. We have also assumed that only human population shed eggs in the soil. The birth rate μ was assumed to be equal to the death rate, hence the total population was kept constant. The number of new infection per susceptible human host, $\lambda(t)$, is given by

$$\lambda(t) = \frac{\beta(W_e + \tau W_l(t))}{1 + aW_e(t) + bW_l(t)}, \tag{3.2}$$

where β is the effective contact rate, a and b are the attacking efficiency rates for the eggs and larva respectively. We assume here that the larva density has a slightly lower probability to initiate new infections, thus, $0 \leq \tau \leq 1$. Individuals in the exposed sub-population E move to the infectious sub-population I at the rate γ. The egg shedding rate for infected humans is represented as ρ. The number of eggs shed by one infected human per day is represented by n_1. In favourable environmental conditions, eggs develop and hatch into infectious larva at the rate α. If the environment is not conducive for an egg to hatch, it degrades in the soil at the rate of σ_1. The larva can only survive in the soil for some time and if no infection occurs, the egg larva dies in the soil at a rate of σ_2. The dynamics of human hosts, worm and larva are represented by the schematic diagram in Figure 3.1.

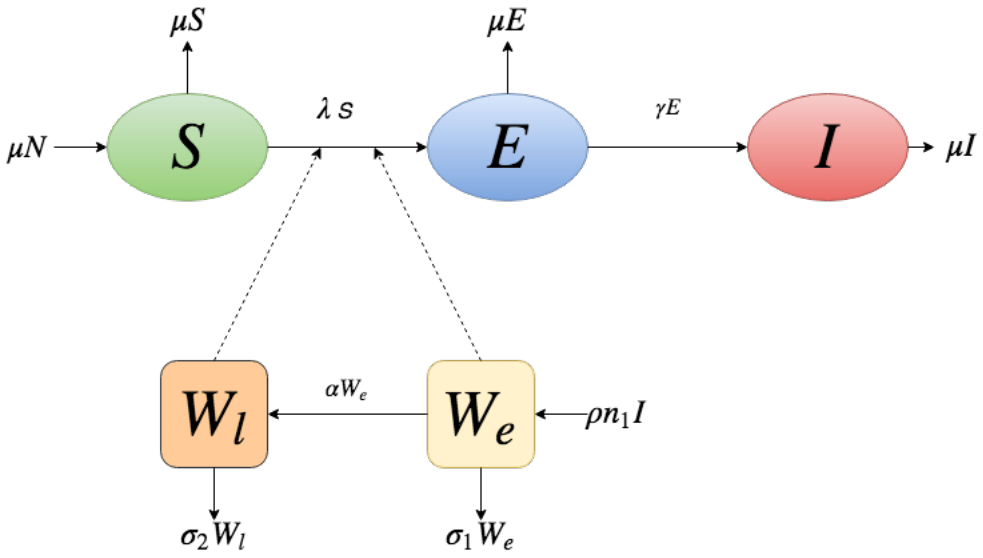

Figure 3.1 A schematic representation of compartmental model.

3.1.1 Model equations

The system (3.3) of nonlinear ordinary differential equations describe the dynamics of soil-transmitted helminths epidemics in human as represented by the scheme in Figure 3.1. The state variables, parameters and initial conditions are considered to be non-negative.

$$\begin{cases} S'(t) &= \mu N(t) - (\lambda + \mu)S(t), \\ E'(t) &= \lambda S(t) - (\mu + \gamma)E(t), \\ I'(t) &= \gamma E(t) - \mu I(t), \\ W_e'(t) &= \rho n_1 I(t) - (\alpha + \sigma_1)W_e(t), \\ W_l'(t) &= \alpha W_e(t) - \sigma_2 W_l(t). \end{cases} \tag{3.3}$$

3.1.2 Model assumptions

1. Birth and death rates are equal.

Variables	Description
$S(t)$	The susceptible human population size.
$E(t)$	The exposed human population size.
$I(t)$	The infectious individuals.
$W_e(t)$	The worm egg population size in the soil.
$W_l(t)$	The worm larva population size in the soil.

Table 3.1 Description of model state variables for the system 3.3.

2. Infection only occurs through infectious larvae or egg ingestion.

3. The eggs are only shed by infectious human hosts.

4. Human host does not acquire immunity against the infection.

5. In-host dynamics of the worm are not considered, therefore worm sexual reproduction is not considered.

6. Low sanitation community is assumed.

7. Eggs density initiate more infections than larva density

3.2 Model analysis.

In this section, we analyse the general properties of the system described by the system (3.3) with non-negative initial conditions. The model describes the dynamics of two interacting populations (humans and larva).

Parameter	Description
μ	Human birth and death rate
β	Larvae-human contact rate.
γ	Rate of progression from latency to actively infectious in humans
ρ	Rate at which eggs are shed by the human population.
n_1	Average number of eggs shed by each individual
α	Rate at which the egg hatches into infectious larva
σ_1	Rate of egg degradation in the soil
σ_1	Rate of larvae degradation in the soil
a	Attacking efficiency rate of the egg
b	Attacking efficiency rate of the larva
τ	Modification parameter

Table 3.2 Description of model parameters as used in the system 3.3

3.2.1 Positivity of solutions

System (3.3) describe the human and worm/egg population. So it is necessary to verify that state variables will be non-negative. Here, we prove that solutions of the system (3.3) with non-negative initial conditions will remain non-negative for all $t \geq 0$.

Theorem 9. *The solutions of system in (3.3) are all non-negative for all $t \geq 0$.*

Proof. From the first equation of system (3.3) we can deduce that,

$$S'(t) = \mu N(t) - (\lambda(t) + \mu)S(t) \geq -(\lambda(t) + \mu)S(t)$$

This inequality ODE can be solved using the method of separation of variables as follows,

$$\frac{dS(t)}{S(t)} \geq -(\lambda(t) + \mu)dt$$
$$\int_{S(0)}^{S(t)} \frac{dP}{P} \geq -\int_0^t (\lambda(y) + \mu)dy$$

And this integrates to

$$S(t) \geq S(0)\mathbf{exp}\Big(-\int_0^t (\lambda(y) + \mu)dy\Big) \geq 0.$$

Similarly for other equations of system (3.3) we deduce that,

$$E(t) \geq E(0)\mathbf{exp}(-(\mu + \gamma)dt) > 0$$
$$I(t) \geq I(0)\mathbf{exp}(-\mu dt) > 0$$
$$W_e(t) \geq W_e(0)\mathbf{exp}(-(\alpha + \sigma_1)dt) > 0$$
$$W_l(t) \geq W_l(0)\mathbf{exp}(-\sigma_2 dt) > 0$$

Thus, the solutions of system (3.3) remain positive for $t \geq 0$. □

3.2.2 Invariant region

Lemma 1. *The solutions of system (3.3) are uniformly bounded in the set* $\Omega = \Omega_1 \times \Omega_2$*, where*

$$\Omega_1 = \Big\{(S(t),E(t),I(t)) \in \mathbb{R}^3_+ : N(t) \leq N_0\Big\},$$
$$\Omega_2 = \Big\{(W_e(t),W_l(t)) \in \mathbb{R}^2_+ : W_e \leq \frac{\rho n_1 N_0}{\alpha+\sigma_1}, \quad W_l \leq \frac{\alpha\rho n_1 N_0}{\alpha+\sigma_1}\Big\}.$$

Proof. The rate of change of the human population is given by

$$\frac{dN(t)}{dt} = 0.$$

Therefore the total population is constant,

$$N(t) = N_0,$$

which means as $t \to \infty$, $0 \leq N(t) \leq N_0$.

Since the total human population is constant, we know that $I(t) \leq N_0$ which implies that,

$$\begin{aligned} &\frac{dW_e(t)}{dt} \leq \rho n_1 N_0 - (\alpha+\sigma_1)W_e(t), \\ &\frac{dW_e(t)}{dt} + (\alpha+\sigma_1)W_e(t) \leq \rho n_1 N_0. \end{aligned} \tag{3.4}$$

This ODE can be solved by finding integrating factor:

$$F(t) = \mathbf{exp}(\int(\alpha+\sigma_1)dt) = \mathbf{exp}((\alpha+\sigma_1)t) \tag{3.5}$$

Multiplying Equation (3.4) and (3.5) gives

$$\frac{dW_e(t)}{dt}\mathbf{exp}((\alpha+\sigma_1)t) + (\alpha+\sigma_1)W_e\mathbf{exp}((\alpha+\sigma_1)t) \leq \rho n_1 N_0\mathbf{exp}((\alpha+\sigma_1)t). \tag{3.6}$$

Equation (3.6) can be re-written as

$$\frac{d}{dt}(W_e(t)\mathbf{exp}(\alpha+\sigma_1)t) \leq \rho n_1 N_0\mathbf{exp}((\alpha+\sigma_1)t).$$

Integrating both sides and using the Fundamental Theorem of Calculus [35]

$$W_e(t) \leq \frac{\rho n_1 N_0}{\alpha+\sigma_1} + \frac{C}{\mathbf{exp}((\alpha+\sigma_1)t)}$$

And the constant term C can be solved using initial condition $W_e(0)$ which gives the solution:

$$W_e(t) \leq \left(W_e(0) - \frac{\rho n_1 N_0}{\alpha+\sigma_1}\right)\mathbf{exp}(-(\alpha+\sigma_1)t) + \frac{\rho n_1 N_0}{\alpha+\sigma_1} \tag{3.7}$$

As $t \to \infty$ the eggs population size in the soil remains in the interval

$$W_e(0) \leq W_e(t) \leq \frac{\rho n_1 N_0}{\alpha+\sigma_1} \tag{3.8}$$

And therefore the population of eggs in the soil, $W_e(t)$, is bounded in the first orthant.

For the larvae population we can use the results given by Equation (3.8) and the fifth equation of our system (3.3) and notice that

$$\frac{dW_l(t)}{dt} + \sigma_2 W_l(t) \leq \frac{\alpha\rho n_1 N_0}{\alpha+\sigma_1}$$

This can also be solved using integrating factor and differential inequality

$$F(t) = \mathbf{exp}\Big(\int \sigma_2 dt\Big) = \mathbf{exp}(\sigma_2 t) \tag{3.9}$$

which solves to:

$$W_l(t) \leq \left(W_l(0) - \frac{\alpha\rho n_1 N_0}{(\alpha+\sigma_1)\sigma_2}\right)\mathbf{exp}(-\sigma_2 t) + \frac{\alpha\rho n_1 N_0}{(\alpha+\sigma_1)\sigma_2}$$

Also for larva, as $t \to \infty$ the infectious larva population size, W_l, in the soil remains in the interval

$$W_l(0) \leq W_l(t) \leq \frac{\alpha\rho n_1 N_0}{(\alpha+\sigma_1)\sigma_2}.$$

We can, therefore, conclude that the human, egg and larva population will approach the threshold N, $\frac{\rho n_1 N_0}{\alpha+\sigma_1}$ and $\frac{\alpha\rho n_1 N_0}{(\alpha+\sigma_1)\sigma_2}$ respectively as $t \to \infty$. Therefore, all the solutions starting in the region Ω remain in Ω. And then the region is attracting. Thus Ω is a feasible region for the system (3.3). □

3.2.3 Disease free equilibrium

When there is no disease in the population the disease-free equilibrium point (DFE) exists. The model we are studying assume that the birth and death rate are equal, therefore the total population is constant throughout. The disease-free equilibrium is therefore only possible when the whole population is susceptible and no parasitic larva and eggs are present in the soil. The DFE for our system (3.3) is given by

$$E_0 = (N, 0, 0, 0, 0).$$

3.2.4 The basic reproduction number

The basic reproduction number is the number of secondary infections caused by the introduction of one infectious case in the wholly susceptible population. This quantity is important in the epidemiological study to asses the spread of the disease. For the system (3.3), we calculate the basic reproduction number using the next generation matrix method described in chapter 1 and [36]. We consider the matrix $\mathscr{F}$ consisting of rates of appearance of new infections in the model

$$\mathscr{F} = \begin{pmatrix} \frac{\beta(W_e(t)+\tau W_l(t))S(t)}{1+aW_e(t)+bW_l(t)} \\ 0 \\ 0 \\ 0 \end{pmatrix}.$$

The Jacobian matrix of $\mathscr{F}$ at the disease-free equilibrium, E_0 is given by

$$\begin{pmatrix} 0 & 0 & \beta N_0 & \beta\tau N_0 \\ 0 & 0 & 0 & 0 \\ 0 & 0 & 0 & 0 \\ 0 & 0 & 0 & 0 \end{pmatrix}.$$

Now, we consider the transition matrix, $\mathscr{V}$,

$$\mathscr{V} = \begin{pmatrix} (\mu+\gamma)E(t) \\ \mu I(t) - \gamma E(t) \\ (\alpha+\sigma_1)W_e(t) - \rho n_1 I(t) \\ \sigma_2 W_l(t) - \alpha W_e(t) \end{pmatrix}.$$

The Jacobian matrix of $\mathscr{V}$ at the disease-free equilibrium, E_0, is given as follows

$$V = \begin{pmatrix} \mu+\gamma & 0 & 0 & 0 \\ -\gamma & \mu & 0 & 0 \\ 0 & -\rho n_1 & \alpha+\sigma_1 & 0 \\ 0 & 0 & -\alpha & \sigma_2 \end{pmatrix}.$$

The inverse of matrix V is given by

$$V^{-1} = \begin{pmatrix} \frac{1}{\gamma+\mu} & 0 & 0 & 0 \\ \frac{\gamma}{\mu(\gamma+\mu)} & \frac{1}{\mu} & 0 & 0 \\ \frac{\gamma\rho n_1}{(\gamma+\mu)(\alpha+\sigma_1)\mu} & \frac{\rho n_1}{\mu(\alpha+\sigma_1)} & \frac{1}{\alpha+\sigma_1} & 0 \\ \frac{\alpha\gamma\rho n_1}{\sigma_2(\alpha+\sigma_1)(\gamma+\mu)\mu} & \frac{\alpha\rho n_1}{\sigma_2(\alpha+\sigma_1)\mu} & \frac{\alpha}{\sigma_2(\alpha+\sigma_1)} & \frac{1}{\sigma_2} \end{pmatrix}.$$

The next generation matrix FV^{-1} is given by

$$FV^{-1} = \begin{pmatrix} \frac{\beta\gamma\rho n_1 N_0(\alpha\tau+\sigma_2)}{\sigma_2(\alpha+\sigma_1)(\gamma+\mu)\mu} & \frac{\beta\rho n_1 N_0(\alpha\tau+\sigma_2)}{\sigma_2(\alpha+\sigma_1)\mu} & \frac{\beta N_0(\alpha\tau+\sigma_2)}{\sigma_2(\alpha+\sigma_1)} & \frac{\beta\tau N_0}{\sigma_2} \\ 0 & 0 & 0 & 0 \\ 0 & 0 & 0 & 0 \\ 0 & 0 & 0 & 0 \end{pmatrix}.$$

The reproduction number is the spectral radius of the next generation matrix FV^{-1} and it is given by

$$R_0 = \frac{\beta\gamma\rho n_1 N_0(\alpha\tau+\sigma_2)}{\sigma_2(\gamma+\mu)(\alpha+\sigma_1)\mu}. \tag{3.10}$$

The effect of the model parameter in the reproduction number.

We calculate the change in the basic reproduction caused by the model parameters $\beta, \rho, n_1, \gamma, \sigma_1, \alpha$ and σ_2, we compute the partial derivative of equation (3.10) with respect to the model parameter

$$\begin{aligned}
\frac{\partial R_0}{\partial \beta} &= \frac{\alpha\gamma\rho n_1 N_0(\alpha\tau+\sigma_2)}{\sigma_2(\gamma+\mu)(\alpha+\sigma_1)\mu},\\
\frac{\partial R_0}{\partial \rho} &= \frac{\beta\alpha\gamma n_1 N_0(\alpha\tau+\sigma_2)}{\sigma_2(\gamma+\mu)(\alpha+\sigma_1)\mu},\\
\frac{\partial R_0}{\partial n_1} &= \frac{\beta\alpha\gamma\rho N_0(\alpha\tau+\sigma_2)}{\sigma_2(\gamma+\mu)(\alpha+\sigma_1)\mu},\\
\frac{\partial R_0}{\partial \gamma} &= \frac{\beta\rho n_1 N_0(\alpha\tau+\sigma_2)}{(\gamma+\mu)^2(\alpha+\sigma_1)\sigma_2},\\
\frac{\partial R_0}{\partial \sigma_1} &= -\frac{\beta\rho n_1 N_0(\alpha\tau+\sigma_2)}{\mu(\gamma+\mu)(\alpha+\sigma_1)^2\sigma_2},\\
\frac{\partial R_0}{\partial \alpha} &= \frac{\beta\rho n_1 N_0(\tau\sigma_1-\sigma_2)}{\mu(\gamma+\mu)(\alpha+\sigma_1)^2\sigma_2},\\
\frac{\partial R_0}{\partial \sigma_2} &= -\frac{\beta\rho n_1\tau N_0}{\mu(\gamma+\mu)(\alpha+\sigma_1)\sigma_2^2}.
\end{aligned}$$

$\frac{\partial R_0}{\partial \beta}, \frac{\partial R_0}{\partial \rho}, \frac{\partial R_0}{\partial n_1}, \frac{\partial R_0}{\partial \gamma}$ being positive means that the basic reproduction number, R_0, increases with the parameters rate β, ρ, n_1, γ. Biologically, we expect that the increase contact rate, human egg shedding rate, average number of eggs shed by each individual and progression rate from latency to actively infectious will increase the number of infections produced because of an infectious individual introduced into the population. We therefore conclude that the interventions aiming the contact rate reduces, egg shedding rate, progression rate and the average number of eggs shed by each individual reduces the number of new infections. On the other hand, an increase in the egg and larva degradation rate σ_1 and σ_2 respectively is expected to decrease the number of new infections.

3.2.5 Existence of endemic equilibrium

At the endemic equilibrium point (EEP), humans are infected by the STH larvae. The endemic equilibrium of the model under study is given by

$$E_1 = (S^*, E^*, I^*, W_e^*, W_l^*),$$

satisfying the following equations

$$\begin{aligned} \mu N^*(t) - (\lambda + \mu) S^*(t) &= 0, \\ \lambda S^*(t) - (\mu + \gamma) E^*(t) &= 0, \\ \gamma E^*(t) - \mu I^*(t) &= 0, \\ \rho n_1 I^*(t) - (\alpha + \sigma_1) W_e^*(t) &= 0, \\ \alpha W_e^*(t) - \sigma_2 W_l^*(t) &= 0. \end{aligned} \tag{3.11}$$

The EEP, E_1 is calculated by solving the equations in (3.11). The first equation in the set of equations in (3.11) yielded

$$S^* = \frac{\mu N_0}{\lambda^* + \mu}, \tag{3.12}$$

Similarly for the rest of the equations,

$$E^* = \frac{\lambda^* \mu N_0}{(\mu + \gamma)(\lambda^* + \mu)}, \tag{3.13}$$

$$I^* = \frac{\gamma \lambda^* N_0}{(\mu + \gamma)(\lambda^* + \mu)}, \tag{3.14}$$

$$W_e^* = \frac{\rho n_1 \gamma \lambda^* N_0}{(\mu + \gamma)(\lambda^* + \mu)(\alpha + \sigma_1)}, \tag{3.15}$$

$$W_l^* = \frac{\alpha \rho n_1 \gamma \lambda^* N_0}{\sigma_2 (\mu + \gamma)(\lambda^* + \mu)(\alpha + \sigma_1)}. \tag{3.16}$$

The equations (3.12) - (3.16) can be written as the basic reproduction number as follows

$$S^* = \frac{(\gamma+\mu)(\alpha+\sigma_1)\sigma_2(\beta+b\mu(\mu-\alpha\tau)+\mu R_0)(b\alpha\tau+a\sigma_2)}{\beta\gamma\rho n_1(\alpha\tau+\sigma_2)(\beta+b\mu^2+a\mu\sigma_2)\mu}, \tag{3.17}$$

$$E^* = \frac{\sigma_2\mu(\alpha+\sigma_1)}{\gamma\rho n_1(\beta+\mu(a\sigma_2+b\mu))}(R_0-1), \tag{3.18}$$

$$I^* = \frac{\sigma_2\mu(\alpha+\sigma_1)}{\rho n_1(\beta+\mu(a\sigma_2+b\mu))}(R_0-1), \tag{3.19}$$

$$W_e^* = \frac{\sigma_2\mu}{\beta+\mu(a\sigma_2+b\mu)}(R_0-1), \tag{3.20}$$

$$W_l^* = \frac{\alpha\mu}{\beta+\mu(a\sigma_2+b\mu)}(R_0-1). \tag{3.21}$$

We note from the equations (3.17) - (3.21) that the endemic equilibrium point exists only when $R_0 > 1$.

3.2.6 Stability analysis of disease-free equilibrium.

The system (3.3) always has a disease-free equilibrium E_0. The disease-free equilibrium corresponds to the model condition of no STH breakout.

Theorem 10. *The disease free equilibrium for the system (3.3) exist; and it is locally asymptotically stable in the set* Ω *if* $R_0 < 1$ *and unstable otherwise.*

Proof. The Jacobian matrix of system (3.3) evaluated at DFE is given by

$$J(E_0) = \begin{pmatrix} -\mu & 0 & 0 & \beta N_0 & -\beta\tau N_0 \\ 0 & -(\mu+\gamma) & 0 & \beta N_0 & \beta\tau N_0 \\ 0 & \gamma & -\mu & 0 & 0 \\ 0 & 0 & \rho n_1 & -(\alpha+\sigma_1) & 0 \\ 0 & 0 & 0 & \alpha & -\sigma_2 \end{pmatrix}. \tag{3.22}$$

The eigenvalues of the Jacobian matrix in (3.22) are $x_1 = -\mu$ and the rest are solutions of the equation

$$a_4 + a_3 x + a_2 x^2 + a_1 x^3 + x^4 = 0. \tag{3.23}$$

The coefficients of the characteristic equation in (3.23) are;

$$\begin{aligned}
a_1 &= \alpha + \gamma + 2\mu + \sigma_1 + \sigma_2 > 0,\\
a_2 &= \mu(\gamma+\mu) + \alpha(\gamma+2\mu) + (\alpha+\gamma+2\mu)\sigma_2 + (\gamma+2\mu+\sigma_2)\sigma_1 > 0,\\
a_3 &= \mu(\gamma+\mu)(\alpha+\sigma_1) + (\mu(\gamma+\mu) + \alpha(\gamma+2\mu) + (\gamma+2\mu)\sigma_1)\sigma_2,\\
a_4 &= \frac{1}{\mu(\alpha+\sigma_1)(\gamma+\mu)\sigma_2}(1-R_0).
\end{aligned}$$

According to the Descartes rule of signs, if $R_0 < 1$ there will be no sign change in the coefficients of the characteristics equation in (3.23). Therefore, there are no positive eigenvalues when $R_0 < 1$. □

Theorem 11. *The disease free equilibrium is globally asymptotically stable in the positive invariant region if* $R_0 \leq 1$.

Proof. We define the candidate Lyapunov function as

$$L(t) = \sigma_2 E + \frac{\sigma_2(\mu+\gamma)}{\gamma} I + \frac{\mu(\mu+\gamma)\sigma_2}{\rho n_1 \gamma} W_e + \beta W_l. \tag{3.24}$$

The time derivative of (3.24) is given by

$$\begin{aligned}
\frac{dL}{dt} &= \sigma_2 \frac{dE}{dt} + \frac{\sigma_2(\mu+\gamma)}{\gamma}\frac{dI}{dt} + \frac{\mu(\mu+\gamma)\sigma_2}{\rho n_1 \gamma}\frac{dW_e}{dt} + \beta\frac{dW_l}{dt},\\
&= \sigma_2(\beta(W_e+W_l) - (\mu+\gamma)E(t)) + \frac{\sigma_2(\mu+\gamma)}{\gamma}(\gamma E(t) - \mu I(t))\\
&+ \frac{\mu(\mu+\gamma)\sigma_2}{\rho n_1 \gamma}(\rho n_1 I(t) - (\alpha+\sigma_1)W_e(t)) + \beta(\alpha W_e(t) - \sigma_2 W_l(t)),\\
&= \Big(\frac{\mu(\mu+\gamma)(\alpha+\sigma_1)\sigma_2}{\rho n_1 \gamma}(R_0 - 1)\Big) W_e(t).
\end{aligned} \tag{3.25}$$

From 3.25 we can clearly see that $\frac{dL}{dt} < 0$ for $R_0 < 1$. And also, $\frac{dL}{dt} = 0$ if and only if $E = I = W_e = W_i = 0$. Therefore L is the Lypunov function. Therefore the largest possible invariant set in $\left\{(S,E,I,W_e,W_l) \in \Omega : \frac{dL}{dt} = 0\right\}$ is the singleton $\{E_0\}$. According to La-Salle's invariant principle E_0 is globally attractive. Therefore the disease-free equilibrium is globally asymptotically stable for $R_0 < 1$. □

3.2.7 Stability analysis of endemic equilibrium.

From the calculations in section 3.2.5, we know that the system described in (3.3) has the unique endemic equilibrium E_1. The endemic equilibrium means the disease does not die when introduced into the population and all the states of the model reach the stable state. In this section, we investigate the stability of the endemic equilibrium point.

Theorem 12. *The endemic equilibrium point E_1 is locally asymptotically stable in the region Ω if $R_0 > 1$.*

Proof. We used the centre manifold theorem to study the stability of the endemic equilibrium. For simplicity let re-define state variables $S = x_1, E = x_2, I = x_3, W_e = x_4$ and $W_l = x_5$. Therefore, we can re-write system (3.3) as

$$\frac{dx_i}{dt} = f(x_i,t) \quad \text{for} \quad i = 1,2,3,4,5 \tag{3.26}$$

Thus the system (3.3) can be rewritten as follows

$$\begin{cases} x_1'(t) &= \mu N(t) - (\lambda+\mu)x_1(t), \\ x_2'(t) &= \lambda x_1(t) - (\mu+\gamma)x_2(t), \\ x_3'(t) &= \gamma x_2(t) - \mu x_3(t), \\ x_4'(t) &= \rho n_1 x_3(t) - (\alpha+\sigma_1)x_4(t), \\ x_5'(t) &= \alpha x_4(t) - \sigma_2 x_5(t). \end{cases} \tag{3.27}$$

$R_0 = 1$ is similar to having

$$\beta = \beta^* = \frac{\sigma_2(\gamma+\mu)(\alpha+\sigma_1)\mu}{\alpha\gamma\rho n_1 N_0(\alpha\tau+\sigma_2)}.$$

where β^* is chosen to be the bifurcation parameter when $R_0 = 1$.

The Jacobian matrix of the system (3.27) at DFE with $\beta = \beta^*$ is given by

$$J(E_0,\beta^*) = \begin{pmatrix} -\mu & 0 & 0 & \beta^* N_0 & -\beta^*\tau N_0 \\ 0 & -(\mu+\gamma) & 0 & \beta^* N_0 & \beta^*\tau N_0 \\ 0 & \gamma & -\mu & 0 & 0 \\ 0 & 0 & \rho n_1 & -(\alpha+\sigma_1) & 0 \\ 0 & 0 & 0 & \alpha & -\sigma_2 \end{pmatrix}. \tag{3.28}$$

The linearised system $J(E_0)$ evaluated in (3.22) is similar to $J(E_0,\beta^*)$ evaluated at $R_0 = 1$, hence the characteristics polynomial $a_3x + a_2x^2 + a_1x^3 + x^4 = 0$ has the eigenvalues $x_1 = 0$ and $x_2 = -\mu$. We also recall from section (3.2.6) that the constants a_1, a_2 and a_3 are all positive and concluded using the Descartes rule of signs that other roots (eigenvalues) of the characteristics equations are negative. Since we have a simple zero eigenvalue, we can apply the centre manifold theorem to assess local stability of the endemic equilibrium by defining the left eigenvector associated zero eigenvalue as

$$\mathbf{w} = (w_1, w_2, w_3, w_4, w_5),$$

and the left eigenvector can be calculated by solving the equation

$$\mathbf{w}[J(E_0,\beta^*)] = 0,$$

$$(w_1, w_2, w_3, w_4, w_5)\begin{bmatrix} -\mu & 0 & 0 & -\beta^* N_0 & -\beta^*\tau N_0 \\ 0 & -(\mu+\gamma) & 0 & \beta^* N_0 & \beta^*\tau N_0 \\ 0 & \gamma & -\mu & 0 & 0 \\ 0 & 0 & \rho n_1 & -(\alpha+\sigma_1) & 0 \\ 0 & 0 & 0 & \alpha & -\sigma_2 \end{bmatrix} = 0,$$

which solves to

$$(w_1,w_2,w_3,w_4,w_5)=\Big(0,\frac{\sigma_2}{\beta^*\tau N_0}w_5,\frac{\sigma_2(\mu+\gamma)}{\beta^*\tau N_0\gamma}w_5,\frac{\sigma_2(\mu+\gamma)\mu}{\beta^*\tau N_0\gamma\rho n_1}w_5,w_5\Big).$$

We also define the right eigenvector associated with the zero eigenvalue as

$$\mathbf{v}=(v_1,v_2,v_3,v_4,v_5),$$

and it can be calculated by solving the equation

$$[J(E_0,\beta^*)]\mathbf{v}^T=0,$$

$$\begin{pmatrix}-\mu & 0 & 0 & 0 & -\beta^*N_0\\ 0 & -(\mu+\gamma) & 0 & 0 & \beta^*N_0\\ 0 & \gamma & -\mu & 0 & 0\\ 0 & 0 & \rho n_1 & -(\alpha+\sigma_1) & 0\\ 0 & 0 & 0 & \alpha & -\sigma_2\end{pmatrix}\begin{pmatrix}v_1\\ v_2\\ v_3\\ v_4\\ v_5\end{pmatrix}=0,$$

which solves to

$$(v_1,v_2,v_3,v_4,v_5)=\Big(-\frac{\beta^*N_0(\sigma_2+\tau)}{\mu\alpha}v_5,\frac{\sigma_2(\alpha+\sigma_1)\mu}{\alpha\gamma\rho n_1}v_5,\frac{\sigma_2(\alpha+\sigma_1)}{\alpha n_1}v_5,\frac{\sigma_2}{\alpha}v_5,v_5\Big)$$

Now we will compute the value of a and b as described in Theorem 7. Since $w_1=0$ we will only computed the partial derivatives for f_2,f_3,f_4 and f_5. The partial derivatives at the disease free equilibrium are given by

$$\frac{\partial^2 f_2}{\partial x_1\partial x_5}=\frac{\partial^2 f_2}{\partial x_5\partial x_1}=\beta^*\tau,\quad \frac{\partial^2 f_2}{\partial x_5\partial x_5}=-2\beta^*N_0b\tau \tag{3.29}$$

$$\frac{\partial^2 f_2}{\partial x_1\partial x_4}=\frac{\partial^2 f_2}{\partial x_4\partial x_1}=\beta^*,\quad \frac{\partial^2 f_2}{\partial x_4\partial x_4}=-2\beta^*N_0a \tag{3.30}$$

$$\frac{\partial^2 f_2}{\partial x_4\partial x_5}=\frac{\partial^2 f_2}{\partial x_5\partial x_4}=-\beta^*N_0(a\tau+b) \tag{3.31}$$

$$\frac{\partial f_2}{\partial x_4\partial\beta^*}=N_0,\quad \frac{\partial f_2}{\partial x_5\partial\beta^*}=N_0\tau \tag{3.32}$$

The value of a and b is given by

$$a = -\frac{2\sigma_2}{\alpha^2\tau\mu}((\sigma_2+\tau)(\beta^*\sigma_2+a\tau+2a\sigma_2\mu)a\sigma_2^2\mu)w_5v_5^2 < 0 \tag{3.33}$$

$$b = \frac{\sigma_2(\alpha+\sigma_2)}{\alpha\beta^*\tau}w_5v_5 > 0 \tag{3.34}$$

Therefore $a < 0$, $b > 0$ and there exist a forward bifurcation at $R_0 = 1$ and this implies that the endemic equilibrium point E_1 is locally asymptotically stable for $R_0 > 1$ but close to one. □

Theorem 13. *The endemic equilibrium is globally asymptotically stable when* $R_0 > 1$.

Proof. Let define the Lyapunov function

$$L = \sum_{i=1}^{5} D_iL_i, \quad D_i > 0,$$

where

$$L_i = x - x^* - x^* \ln\left(\frac{x_i}{x_i^*}\right), \quad x_i \in \{S,E,I,W_e,W_o\}.$$

Equating the partial differentiation of L to zero, that is

$$\frac{\partial L_i}{\partial x_i} = D_i\left(1-\frac{x_i^*}{x_i}\right) = 0,$$

yield that $x_i = x_i^*$ which means $S = S^*$, $E = E^*$, $I = I^*$, $W_e = W_e^*$ and $W_l = W_l^*$ implying that the endemic equilibrium is the only stationary point for L. Moreover,

$$\frac{\partial^2 L_i}{\partial x^2} = D_i\frac{x_i^*}{x_i^2} > 0,$$

implies that E_1 is the global minimum for L. Differentiating L with respect to time yields

$$\frac{dL}{dt} = \sum_{i=1}^{3} D_i\left(1-\frac{x_i^*}{x_i}\right)\frac{dx_i}{dt} + D_4\left(1-\frac{x_4^*}{x_4}\right)\frac{dx_4}{dt} + D_5\left(1-\frac{x_5^*}{x_5}\right)\frac{dx_5}{dt}. \tag{3.35}$$

We know that

$$N \le N_0, \tag{3.36}$$

$$W_e(t) \le \left(W_e(0) - \frac{\rho n_1 N_0}{\alpha+\sigma_1}\right)e^{-(\alpha+\sigma_1)t} + \frac{\rho n_1 N_0}{\alpha+\sigma_1}, \tag{3.37}$$

$$W_l(t) \le \left(W_l(0) - \frac{\alpha\rho n_1 N_0}{(\alpha+\sigma_1)\sigma_2}\right)e^{-\sigma_2 t} + \frac{\alpha\rho n_1 N_0}{(\alpha+\sigma_1)\sigma_2}. \tag{3.38}$$

Differentiating Equations (3.36), (3.37) and (3.38) with respect to time gives

$$\frac{dN}{dt} \leq 0, \tag{3.39}$$

$$\frac{dW_e}{dt} \leq (\alpha+\sigma_1)\left(\frac{\rho n_1 N_0}{\alpha+\sigma_1} - W_e(0)\right)e^{-(\alpha+\sigma_1)t} \tag{3.40}$$

$$\frac{dW_l}{dt} \leq \sigma_2\left(\frac{\alpha\rho n_1 N_0}{(\alpha+\sigma_1)\sigma_2} - W_l(0)\right)e^{-\sigma_2 t} \tag{3.41}$$

It follows that

$$\begin{aligned}\frac{dL}{dt} \leq\ & D_4(\alpha+\sigma_1)\left(1-\frac{x_4^*}{x_4}\right)\left(\frac{\rho n_1 N_0}{\alpha+\sigma_1} - W_e(0)\right)e^{-(\alpha+\sigma_1)t} \\ & + D_5\sigma_2\left(1-\frac{x_5^*}{x_5}\right)\left(\frac{\alpha\rho n_1 N_0}{(\alpha+\sigma_1)\sigma_2} - W_l(0)\right)e^{-\sigma_2 t}.\end{aligned} \tag{3.42}$$

Equation (3.42) clearly shows that if $W_e(0) \leq \frac{\rho n_1 N_0}{\alpha+\sigma_1}$ and $W_l(0) \leq \frac{\alpha\rho n_1 N_0}{(\alpha+\sigma_1)\sigma_2}$, $L \leq 0$ and if $W_e(0) \geq \frac{\rho n_1 N_0}{\alpha+\sigma_1}$ and $W_l(0) \geq \frac{\alpha\rho n_1 N_0}{(\alpha+\sigma_1)\sigma_2}$, $L \leq 0$ as $t \to \infty$. In addition, $L = 0$ if and only if $S = S^*$, $E = E^*$, $I = I^*$, $W_e = W_e^*$ and $W_l = W_l^*$. Therefore the largest compact invariant set is singleton set E_1 which is endemic equilibrium. By LaSalle's invariant principle E_1 is globally asymptotically stable on Ω. □

3.3 Summary

In this chapter, we formulated and analysed the soil-transmitted helminths model describing the interaction between the parasitic worms and the human population. We proved that the model has positive solutions that are bounded in a biological meaningful region. The basic reproduction number was calculated using the next generation matrix approach. The basic reproduction number was used to assess the contribution of the contact rate β in the dynamics of the disease. Two equilibrium points were computed (disease-free and endemic equilibrium). The analysis revealed that the existence of the endemic equilibrium depends on the value of basic reproduction number R_0.

We further used the Lyapunov function's *LaSalle's* invariance principle to show that the endemic equilibrium is globally asymptotically stable.

Chapter 4

Model With Polynomial Chaos

4.1 Polynomial chaos expansions.

In this section, we consider uncertainty in the model because of environmental and biological disturbances. We, therefore, consider parameters β, γ, ρ and α as functions of random variables depending on the outcome ω of the experiment. The other parameters and initial conditions will not be considered random for simplicity and they can be determined with much more accuracy than one considered as random in this section. The random parameters take the form $\beta(\omega)$, $\gamma(\omega)$, $\rho(\omega)$ and $\alpha(\omega)$. The model state variables $S(t,\omega)$, $E(t,\omega)$, $I(t,\omega)$, $O(t,\omega)$,$L(t,\omega)$ become stochastic processes depending on time and outcome of the experiment [24]. We employ the Generalized polynomial chaos to perform numerical simulations of the dynamics of the model under study with random parameters. Polynomial chaos represent solutions of the system (3.3) and random parameters as the series expansion of orthogonal polynomials in terms of the corresponding random

variables as follows

$$\begin{cases} S(t,\omega) & = \sum_{i=0}^{\infty} S_i(t)\Psi_i((\omega)), \\ E(t,\omega) & = \sum_{i=0}^{\infty} E_i(t)\Psi_i((\omega)), \\ I(t,\omega) & = \sum_{i=0}^{\infty} I_i(t)\Psi_i((\omega)), \\ W_e(t,\omega) & = \sum_{i=0}^{\infty} W_{ei}(t)\Psi_i((\omega)), \\ W_l(t,\omega) & = \sum_{i=0}^{\infty} W_{li}(t)\Psi_i((\omega)), \\ \beta(\omega) & = \sum_{i=0}^{\infty} \beta_i\Psi_i((\omega)), \\ \gamma(\omega) & = \sum_{i=0}^{\infty} \gamma_i\Psi_i((\omega)), \\ \rho(\omega) & = \sum_{i=0}^{\infty} \rho_i\Psi_i((\omega)), \\ \alpha(\omega) & = \sum_{i=0}^{\infty} \alpha_i\Psi_i((\omega)). \end{cases} \tag{4.1}$$

where Ψ_i are carefully selected Lagendre polynomial basis functions.

4.2 Parameters probability distribution

There is no enough information available in literature about the distribution of model random parameters, hence we assume that they all follow the non-informative uniform distribution. Legendre polynomial chaos associated with uniform distribution is therefore chosen as a basis function for expansions given in (4.1), because its weight function matches the distribution of random parameters. This allows the orthogonality of polynomials to be used to make calculations trivial.

For numerical simulations we are going to use Legendre polynomial of order two and chaos dimension of four. There are fifteen Legendre polynomial chaos of degree less or equal to two using

a selection of four. There is one polynomial of degree zero, four of degree one, for each random variable ζ_i, four of degree two in one variable for (ζ_i, ζ_i) and six of degree two, in two variables, each for (ζ_i, ζ_j), $i \neq j$, therefore the number of terms of the polynomial chaos of stochastic process is fifteen, calculated using equation (1.11) as described in Chapter 1.

In practice, a truncated polynomial chaos is considered for computational efficiency. The truncated expansion is given by

$$S(t,\omega) = \sum_{i=0}^{14} S_i(t)\Psi_i((\omega)) = S_0(t) + \sum_{i=1}^{4} S_i(t)\Psi_1(\zeta_i(\omega)) + \sum_{i=1}^{4}\sum_{j=1}^{i} S_{ij}(t)\Psi_2(\zeta_i(\omega),\zeta_j(\omega)) \tag{4.2}$$

$$E(t,\omega) = \sum_{i=0}^{14} E_i(t)\Psi_i((\omega)) = E_0(t) + \sum_{i=1}^{4} E_i(t)\Psi_1(\zeta_i(\omega)) + \sum_{i=1}^{4}\sum_{j=1}^{i} E_{ij}(t)\Psi_2(\zeta_i(\omega),\zeta_j(\omega)) \tag{4.3}$$

$$I(t,\omega) = \sum_{i=0}^{14} I_i(t)\Psi_i((\omega)) = I_0(t) + \sum_{i=1}^{4} I_i(t)\Psi_1(\zeta_i(\omega)) + \sum_{i=1}^{4}\sum_{j=1}^{i} I_{ij}(t)\Psi_2(\zeta_i(\omega),\zeta_j(\omega)) \tag{4.4}$$

$$W_e(t,\omega) = \sum_{i=0}^{14} W_{ei}(t)\Psi_i((\omega)) = W_{e0}(t) + \sum_{i=1}^{4} W_{ei}(t)\Psi_1(\zeta_i(\omega)) + \sum_{i=1}^{4}\sum_{j=1}^{i} W_{eij}(t)\Psi_2(\zeta_i(\omega),\zeta_j(\omega)) \tag{4.5}$$

$$W_l(t,\omega) = \sum_{i=0}^{14} W_{li}(t)\Psi_i((\omega)) = W_{l0}(t) + \sum_{i=1}^{4} W_{li}(t)\Psi_1(\zeta_i(\omega)) + \sum_{i=1}^{4}\sum_{j=1}^{i} W_{lij}(t)\Psi_2(\zeta_i(\omega),\zeta_j(\omega)) \tag{4.6}$$

$(S_0(t), E_0(t), I_0(t), W_{e0}, W_{l0})$ are first-order moments of stochastic processes and Ψ_1, Ψ_2 are Legendre polynomials given as

$$\begin{cases} \Psi_1(\zeta_i(\omega)) & = \zeta_i(\omega), \\ \Psi_2(\zeta_i(\omega), \zeta_i(\omega)) & = \frac{1}{2}(3\zeta_i(\omega)^2 - 1), \\ \Psi_2(\zeta_i(\omega), \zeta_j(\omega)) & = \zeta_i(\omega)\zeta_j(\omega). \end{cases}$$

Random parameters can also be expressed as random variables. Since we are assuming that random variables are independent and identically distributed, each parameter can be represented as a function of only one random variable $(\zeta_1(\omega), \zeta_2(\omega), \zeta_3(\omega), \zeta_4(\omega))$ and functions are given by:

$$\begin{aligned} \beta(\omega) &= \beta_0 + \beta_1\Psi_1(\zeta_1(\omega)) + \beta_2\Psi_2(\zeta_1(\omega), \zeta_1(\omega)), \\ \gamma(\omega) &= \gamma_0 + \gamma_1\Psi_1(\zeta_2(\omega)) + \gamma_2\Psi_2(\zeta_2(\omega), \zeta_2(\omega)), \\ \rho(\omega) &= \rho_0 + \rho_1\Psi_1(\zeta_3(\omega)) + \rho_2\Psi_2(\zeta_3(\omega), \zeta_3(\omega)), \\ \alpha(\omega) &= \alpha_0 + \alpha_1\Psi_1(\zeta_4(\omega)) + \alpha_2\Psi_2(\zeta_4(\omega), \zeta_4(\omega)). \end{aligned}$$

where β_0, γ_0, ρ_0 and α_0 are the first-order moments for each parameter. β_1, γ_1, ρ_1, α_1, β_2, γ_2, ρ_2 and α_2 are constants.

We can now construct the equations used in the numerical simulations. Consider system of differential Equation (3.3) and introducing the truncated polynomial expansions represented by equation (4.2) - (4.6) results:

$$\sum_{i=0}^{14} \frac{dS_i(t)}{dt}\Psi_i(\omega) = \mu N_0 - \sum_{i=0}^{14}\sum_{j=0}^{14}\sum_{k=0}^{14} \beta_i P_j S_k \Psi_i \Psi_j \Psi_k - \mu \sum_{i=0}^{14} S_i \Psi_i \tag{4.7}$$

where

$$P_j = \frac{\sum_{j=0}^{14} W_{ej} + \tau \sum_{j=0}^{14} W_{lj}}{1 + a \sum_{j=0}^{14} W_{ej} + b \sum_{j=0}^{14} W_{lj}} \tag{4.8}$$

We use orthogonality of the basis function to obtain the system of differential equations. Taking

the inner product of (4.7) with basis function.

$$\begin{aligned}\langle \Psi_N, \Psi_N \rangle \frac{dS_N(t)}{dt} = \langle \mu N_0, \Psi_N \rangle - \sum_{i=0}^{14}\sum_{j=0}^{14}\sum_{k=0}^{14} \beta_i P_j S_k \langle \Psi_i \Psi_j \Psi_k, \Psi_N \rangle \\ - \sum_{i=0}^{14} S_i \langle \Psi_i, \Psi_N \rangle\end{aligned} \tag{4.9}$$

The rest of the equations are given as follows

$$\begin{aligned}\langle \Psi_L, \Psi_L \rangle \frac{dE_L(t)}{dt} =& \sum_{i=0}^{14}\sum_{j=0}^{14}\sum_{k=0}^{14} \beta_i P_j S_k \langle \Psi_i \Psi_j \Psi_k, \Psi_N \rangle \\ & - \mu \sum_{i=0}^{14} E_i \langle \Psi_i, \Psi_L \rangle - \sum_{i=0}^{14}\sum_{i=0}^{14} \gamma_i I_j \langle \Psi_i \Psi_j, \Psi_L \rangle\end{aligned} \tag{4.10}$$

$$\langle \Psi_L, \Psi_L \rangle \frac{dI_L(t)}{dt} = \sum_{i=0}^{14}\sum_{i=0}^{14} \gamma_i I_j \langle \Psi_i \Psi_j, \Psi_L \rangle - \mu \sum_{i=0}^{14} I_i \langle \Psi_i, \Psi_L \rangle \tag{4.11}$$

$$\begin{aligned}\langle \Psi_L, \Psi_L \rangle \frac{dW_{eL}(t)}{dt} =& n_1 \sum_{i=0}^{14}\sum_{i=0}^{14} \rho_i I_j \langle \Psi_i \Psi_j, \Psi_L \rangle \\ & - \sum_{i=0}^{14}\sum_{j=0}^{14} \alpha_i W_{ej} \langle \Psi_i \Psi_j, \Psi_L \rangle - \sigma_1 \sum_{i=0}^{14} W_{li} \langle \Psi_i, \Psi_L \rangle\end{aligned} \tag{4.12}$$

$$\langle \Psi_L, \Psi_L \rangle \frac{dW_{lL}(t)}{dt} = \sum_{i=0}^{14}\sum_{i=0}^{14} \alpha_i W_{ej} \langle \Psi_i \Psi_j, \Psi_L \rangle - \sigma_2 \sum_{i=0}^{14} W_{li} \langle \Psi_i, \Psi_L \rangle \tag{4.13}$$

The inner products in the about equations can be calculated using definition 2. Although uncertainty was introduced, equations (4.9) - (4.12) is a system of non-linear ordinary differential equations. This system can be solved numerically using python's ODE solver.

4.3 Mean and Variance

The mean and variance can easily be calculated directly from stochastic Galerkin solutions. Consider the population of infected people $I(t)$ and using definition 9 the mean (E) is given by

$$\begin{aligned}
E(I(t,(\omega))) &= E\left(\sum_{i=0}^{\infty} I_i(t)\Psi_i((\omega))\right) \\
&= \int_{(\omega)} \left(\sum_{i=0}^{\infty} I_i(t)\Psi_i((\omega))\right) f((\omega))d(\omega) \\
&= \sum_{i=0}^{\infty} I_i(t) \int_{(\omega)} \Psi_i((\omega))f(\omega)d(\omega) \\
&= I_0(t) \int_{(\omega)} \Psi_0((\omega))f((\omega))d\omega + \sum_{i=1}^{\infty} I_i(t) \int_{(\omega)} \Psi_i((\omega))f((\omega))d(\omega) \\
&= I_0(t)E(\Psi_0) + \sum_{i=1}^{\infty} I_i(t)E(\Psi_i) \\
E(I(t,\omega)) &= I_0(t)
\end{aligned}$$

by Theorem 3. The variance is given by

$$\begin{aligned}
Var(I(t,\omega)) &= E((I-E(I))^2) \\
&= E\left(\left(\sum_{i=0}^{\infty} I_i(t)\Psi_i((\omega)) - I_0\right)^2\right) \\
&= E\left(\left(\sum_{i=1}^{\infty} I_i(t)\Psi_i((\omega))\right)^2\right) \\
&= \sum_{i=1}^{\infty} I_i^2(t)E(\Psi_i((\omega))^2) \\
&= \sum_{i=1}^{\infty} I_i^2(t)Var(\Psi_i((\omega))) \qquad (4.14)
\end{aligned}$$

Therefore the mean is simply the zero order chaos term and the variance is the sum of squares of the higher order terms. Similarly, we can calculate the mean and variance for all the stochastic

processes. The mean for the rest of the stochastic processes is given by

$$\begin{cases} E(S(t,\omega)) & = S_0(t), \\ E(E(t,\omega)) & = E_0(t), \\ E(W_e(t,\omega)) & = W_{e0}(t), \\ E(W_l(t,\omega)) & = W_{l0}(t), \end{cases} \tag{4.15}$$

and the variance is given by

$$\begin{cases} Var(S(t,\omega)) & = \sum_{i=1}^{\infty} S_i^2(t) Var(\Psi_i((\omega))), \\ Var(E(t,\omega)) & = \sum_{i=1}^{\infty} E_i^2(t) Var(\Psi_i((\omega))), \\ Var(W_e(t,\omega)) & = \sum_{i=1}^{\infty} W_{ei}^2(t) Var(\Psi_i((\omega))), \\ Var(W_l(t,\omega)) & = \sum_{i=1}^{\infty} W_{li}^2(t) Var(\Psi_i((\omega))). \end{cases} \tag{4.16}$$

Noting that the mean is a zero order chaos term and the variance is a sum of squares of higher order terms.

4.4 Sensitivity analysis - Sobol indices

We have shown how to calculate the mean and variance, but it may be useful to calculate how much of variance each uncertain parameter account for. This can be useful in determining parameters responsible for a greater fraction of variance so that more time can be invested in determining that parameter with more certainty to reduce variance. We utilise Sobol indices to study this.

Sobol indices are a decomposition of the model output variance. They determine what fraction of variance each random parameter contribute in the total variance. The truncated variance can be written as:

$$Var(S(t,\omega)) = \sum_{i=1}^{14} I_i^2(t) Var(\Psi_i((\omega))), \tag{4.17}$$

which can be decomposed as follow:

$$\begin{aligned} Var(S(t,\omega) = {} & S_1^2 Var(\Psi_1(\zeta_1(\omega))) + S_2^2 Var(\Psi_1(\zeta_2(\omega))) + S_3^2 Var(\Psi_1(\zeta_3(\omega))) + S_4^2 Var(\Psi_1(\zeta_4(\omega))) \\ & + S_5^2 Var(\Psi_2(\zeta_1(\omega), \zeta_1(\omega))) + S_6^2 Var(\Psi_2(\zeta_2(\omega), \zeta_2(\omega))) \\ & + S_7^2 Var(\Psi_2(\zeta_3(\omega), \zeta_3(\omega))) + S_8^2 Var(\Psi_2(\zeta_4(\omega), \zeta_4(\omega))) \\ & + S_9^2 Var(\Psi_2(\zeta_1(\omega), \zeta_2(\omega))) + S_{10}^2 Var(\Psi_1(\zeta_4(\omega), \zeta_3(\omega))) \\ & + S_{11}^2 Var(\Psi_2(\zeta_1(\omega), \zeta_4(\omega))) + S_{12}^2 Var(\Psi_2(\zeta_2(\omega), \zeta_3(\omega))) \\ & + S_{13}^2 Var(\Psi_2(\zeta_2(\omega), \zeta_4(\omega))) + S_{14}^2 Var(\Psi_2(\zeta_3(\omega), \zeta_4(\omega))) \end{aligned} \tag{4.18}$$

The sobol indices are defined as follows:

$$S_\theta^Y = \frac{V_i + V_{ij}}{Var(Y)} \tag{4.19}$$

where θ and Y is the respective parameter and the state variable respectively. V_i and V_{ij} are the composition of the total variance and stand for the partial first and second order variance respectively. Therefore the sobol indices for susceptible individuals are as follows:

$$\begin{aligned} S_\beta^S &= \frac{S_1^2(t) Var(\Psi_1(\zeta_1(\omega))) + S_5^2(t) Var(\Psi_2(\zeta_1(w), \zeta_1(\omega)))}{Var(S(t,\omega))} \\ S_\gamma^S &= \frac{S_2^2(t) Var(\Psi_1(\zeta_2(\omega))) + S_6^2(t) Var(\Psi_2(\zeta_2(w), \zeta_2(\omega)))}{Var(S(t,\omega))} \\ S_\rho^S &= \frac{S_3^2(t) Var(\Psi_1(\zeta_3(\omega))) + S_7^2(t) Var(\Psi_2(\zeta_3(w), \zeta_3(\omega)))}{Var(S(t,\omega))} \\ S_\alpha^S &= \frac{S_4^2(t) Var(\Psi_1(\zeta_4(\omega))) + S_8^2(t) Var(\Psi_2(\zeta_4(w), \zeta_4(\omega)))}{Var(S(t,\omega))} \end{aligned}$$

Similarly for the rest of the compartments we have, exposed individuals:

$$S_{\beta}^{E} = \frac{E_1^2(t)Var(\Psi_1(\zeta_1(\omega))) + E_5^2(t)Var(\Psi_2(\zeta_1(w),\zeta_1(\omega)))}{Var(E(t,\omega))}$$
$$S_{\gamma}^{E} = \frac{E_2^2(t)Var(\Psi_1(\zeta_2(\omega))) + E_6^2(t)Var(\Psi_2(\zeta_2(w),\zeta_2(\omega)))}{Var(E(t,\omega))}$$
$$S_{\rho}^{E} = \frac{E_3^2(t)Var(\Psi_1(\zeta_3(\omega))) + E_7^2(t)Var(\Psi_2(\zeta_3(w),\zeta_3(\omega)))}{Var(E(t,\omega))}$$
$$S_{\alpha}^{E} = \frac{E_4^2(t)Var(\Psi_1(\zeta_4(\omega))) + E_8^2(t)Var(\Psi_2(\zeta_4(w),\zeta_4(\omega)))}{Var(E(t,\omega))}$$

infectious individuals:

$$S_{\beta}^{I} = \frac{I_1^2(t)Var(\Psi_1(\zeta_1(\omega))) + I_5^2(t)Var(\Psi_2(\zeta_1(w),\zeta_1(\omega)))}{Var(I(t,\omega))}$$
$$S_{\gamma}^{I} = \frac{I_2^2(t)Var(\Psi_1(\zeta_2(\omega))) + I_6^2(t)Var(\Psi_2(\zeta_2(w),\zeta_2(\omega)))}{Var(I(t,\omega))}$$
$$S_{\rho}^{I} = \frac{I_3^2(t)Var(\Psi_1(\zeta_3(\omega))) + I_7^2(t)Var(\Psi_2(\zeta_3(w),\zeta_3(\omega)))}{Var(I(t,\omega))}$$
$$S_{\alpha}^{I} = \frac{I_4^2(t)Var(\Psi_1(\zeta_4(\omega))) + I_8^2(t)Var(\Psi_2(\zeta_4(w),\zeta_4(\omega)))}{Var(I(t,\omega))}$$

egg density in the soil:

$$S_{\beta}^{W_e} = \frac{W_{e1}^2(t)Var(\Psi_1(\zeta_1(\omega))) + W_{e5}^2(t)Var(\Psi_2(\zeta_1(w),\zeta_1(\omega)))}{Var(W_e(t,\omega))}$$
$$S_{\gamma}^{W_e} = \frac{W_{e2}^2(t)Var(\Psi_1(\zeta_2(\omega))) + W_{e6}^2(t)Var(\Psi_2(\zeta_2(w),\zeta_2(\omega)))}{Var(W_e(t,\omega))}$$
$$S_{\rho}^{W_e} = \frac{W_{e3}^2(t)Var(\Psi_1(\zeta_3(\omega))) + W_{e7}^2(t)Var(\Psi_2(\zeta_3(w),\zeta_3(\omega)))}{Var(W_e(t,\omega))}$$
$$S_{\alpha}^{W_e} = \frac{W_{e4}^2(t)Var(\Psi_1(\zeta_4(\omega))) + W_{e8}^2(t)Var(\Psi_2(\zeta_4(w),\zeta_4(\omega)))}{Var(W_e(t,\omega))}$$

larvae density in the soil:

$$S_{\beta}^{W_l} = \frac{W_{l1}^2(t)Var(\Psi_1(\zeta_1(\omega))) + W_{l5}^2(t)Var(\Psi_2(\zeta_1(w),\zeta_1(\omega)))}{Var(W_l(t,\omega))}$$
$$S_{\gamma}^{W_l} = \frac{W_{l2}^2(t)Var(\Psi_1(\zeta_2(\omega))) + W_{l6}^2(t)Var(\Psi_2(\zeta_2(w),\zeta_2(\omega)))}{Var(W_l(t,\omega))}$$
$$S_{\rho}^{W_l} = \frac{W_{l3}^2(t)Var(\Psi_1(\zeta_3(\omega))) + W_{l7}^2(t)Var(\Psi_2(\zeta_3(w),\zeta_3(\omega)))}{Var(W_l(t,\omega))}$$
$$S_{\alpha}^{W_l} = \frac{W_{l4}^2(t)Var(\Psi_1(\zeta_4(\omega))) + W_{l8}^2(t)Var(\Psi_2(\zeta_4(w),\zeta_4(\omega)))}{Var(W_l(t,\omega))}$$

4.5 Summary

In this chapter, we introduced uncertainty in parameters governing the model formulated in chapter 3. Contact rate β, progression rate γ, egg shedding rate ρ and egg hatching rate α were assumed to be random. These parameters were then re-written as the functions of random variables with probability distributions. Parameters were assumed to follow a uniform distribution, due to the lack of data points to establish a suitable distribution for each parameter. The mean and variance were calculated directly from the stochastic solutions of the model. We found that the mean is the zero order chaos term and the variance is the sum of squares of the higher order terms. The Sobol indices were calculated by decomposing the variance to find the influence of each parameter in the variance. Sobol indices are used to determine the parameter responsible for the majority of variance so that most resources could be used in determining that parameter with more certainty.

Chapter 5

Numerical results

5.1 Introduction

In chapter 3, we formulated and analysed a model analytically to enhance the understanding of dynamics for soil-transmitted helminths in human hosts interacting with infectious eggs and larva. Furthermore, we introduced randomness in parameters with uncertainty using polynomial chaos for better visualisation of a model with uncertainty parameters in chapter 4. To meet our objective, we employed numerical analysis in the model. Some estimates for parameters were obtained from the literature, while others were estimated from the biological evolution of worm infection. Due to lack of data point to estimate the distribution of random parameters, we assumed they follow a uniform distribution. Therefore simulations presented here are purely theoretical. The open source framework chaospy was use to generate stochastic objects in the model [37] and ODE solver in python was used to solve polynomial chaos coefficients and further determining chaos solution, mean, variance and Sobol indices.

5.2 Parameter Estimation

In this section, we consider average parameter values that encompass features of soil-transmitted helminths (STH) including the rate of infection, incubation period, length of infections period for *ascaris lumbricoides* and hookworm. STH is listed as one of the neglected tropical diseases (NTDs), this makes it a challenge to find parameter values governing our model readily in the literature. Therefore to be able to do numerical simulations, some parameter values would need to be estimated and contextualized. *ascaris lumbricoides* and *trichuris trichiura* have almost similar life cycle. For this reason, our simulations will only focus on *ascaris lumbricoides* and hookworm species.

According to the study of STH in the Nigerian children population, individuals aged between 1 and 17 years were recorded [38]. The birth and death rate is therefore estimated as the reciprocal of the difference in age, which yields $\mu = \frac{1}{16}$ per year. For computational purposes, We have assumed that a year is made up of 365 days.

$\frac{1}{\sigma_1}$ and $\frac{1}{\sigma_2}$ are interpreted as the time spent in the soil by each egg and larvae respectively. $\frac{1}{\sigma_1}$ can be estimated as the average time it takes each egg to develop to become a larva for hookworm. Hookworm egg takes about 9 days to become infectious *filariform* larva, we can therefore estimate that the egg degradation rate as $\sigma_1 = 1/9$ per day [39]. $\frac{1}{\sigma_2}$ is interpreted as the average time each hookworm larva survives in the soil before it infects a human being. Each larva can survive in the soil for about 3 to 5 weeks, assuming the average of 30 days we obtain that $\sigma_2 = \frac{1}{30}$ per day [8]. The average incubation period in humans is about 6 to 7 weeks, assuming the average of 45 days, we obtained that $\gamma = \frac{1}{45}$ per day [8].

World health organisation classify host with moderate intensity of infection to produce between

$2\,000 - 3\,999$ eggs per gram of faeces for hookworm [10]. An average SAC individual excrete an estimate of $96.8 - 127.9$g faeces per day [19]. We used the average of the egg production and faeces mass to estimate the number of eggs produces by one individual, n_1. Therefore the number of hookworm eggs shed by each individual per day is $n_1 = 336\,000$. The hatching rate α is assumed to be the rate a developed egg hatch to be an infectious larva. There is no data in the literature to estimate this parameter and it is mostly dependent on environmental conditions such as temperature and the level of moisture. For this reason, we have assumed that 40% of the eggs hatch into larvae per day, therefore egg hatching rate can be estimated to be $\alpha = 0.4$. The contact rate β could not be estimated using the basic reproduction number simply because most studies estimating the basic reproduction number considers the sexual mating of the worm. We, therefore, assumed that the contact rate depends on the rate of poverty in the particular community and $\beta = 0.0049$ was then estimated using the South African poverty rate. For our model, we assume moderate to high intensity infection as classified by the world health organisation. This class has individuals who shed $2\,000 - 3\,999$ eggs per gram of faeces. Each adult hookworm produces about $15\,000 - 30\,000$ eggs per day. We can then estimate the egg shedding rate $\rho = 0.13$ using these quantities. Similar contextualisation is used for *ascaris lumbricoides* and parameter values are summarised in Table 5.1.

5.3 Initial Conditions

For illustration purposes, we simulated the dynamics of a particular community of $1\,000$ people. Initial the number of susceptible and infectious individuals is 800 and 200 respectively. The initial conditions used in this chapter are summarised in Table 5.2.

Parameter	Hookworm	*Ascaris*	Source
μ	0.0001712	0.0001712	[38]
β	0.0049	0.0049	Estimated
τ	0.33	0	Estimated
a	0	2	Assumed
b	2	0	Assumed
γ	0.0222	0.0133333	[8]
ρ	0.133	0.11	Estimated
n_1	336000	4705000	Estimated
α	0.4	0	Assumed
σ_1	0.11	0.1	[39] [8]
σ_2	0.0333	0.017857	[39] [8]

Table 5.1 Parameter values for hookworm and *ascaris* used in the deterministic simulations. The rates are given in per day.

$S(0)$	$E(0)$	$I(0)$	$W_e(0)$	$W_l(0)$
800	0	200	5000	5000

Table 5.2 Initial conditions used for numerical simulations

5.3.1 The effect of model parameters in the reproduction number

Sobol indices were used to perform the sensitivity analysis of the basic reproduction number to check the parameter values that are significant in the variability of the basic reproduction number.

Figure 5.1 shows the result of the sensitivity analysis from the evaluation of 10 parameters mak-

ing up the reproduction number. The results indicate that parameters β, γ, n_1 and α contributes more in the variability of the basic reproduction number. Therefore interventions addressing these parameters can change the basic reproduction number. The result further reveals that human birth and death rate do not contribute much to the variability of the basic reproduction number. In the analysis of the basic reproduction number in chapter 3, we showed that an increase in the egg degradation rate σ_1 decreases the reproduction number. In figure 5.1 we note that σ_2 is responsible for about 10% variability of the basic reproduction number, so interventions such as soil and plant fumigation can potentially decrease the basic reproduction number.

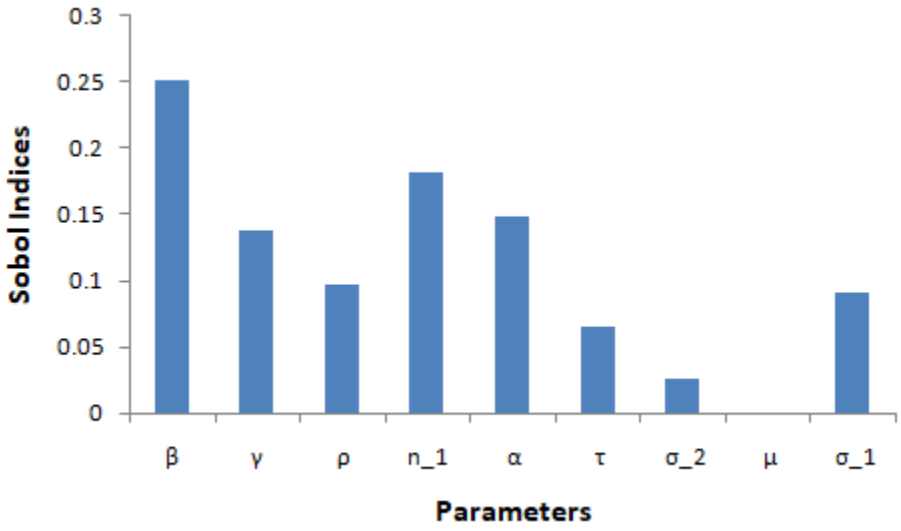

Figure 5.1 A schematic representation of compartmental model.

5.4 Deterministic Model Simulation Results

In this section, we present numerical simulations of the preliminary system represented by system 3.3 to show a clear difference in the model for different hypothetical parameter values. Firstly, we presented simulations for *ascaris* and hookworm species to observe the more prevalent species in the human population. We also varied the contact rate, β, to assess the effect of the human

behaviour in the dynamics of soil-transmitted helminths and presented numerical solutions.

To demonstrate the effect of human behaviour in the dynamics of soil-transmitted helminths, we set the contact rate β to different values. The contact rate β was varied for hookworm, while other parameters were kept the unchanged as given in Table 5.1. The dynamics of human population, larva density and egg density were observed. Figure 5.2 shows the effect of changing the contact rate in the human population, egg density and larva density when β is equalled to 0.039975, 0.029975 and 0.019975. We observe that if the change in β increases, the concentration of egg and larvae increases dramatically. The susceptible population decreases with the increased value of the contact rate β. Exposed group of individuals shows the sharp incline in the peaks followed by a sharp decrease with the increase in β. It was also observed that if the value of β increased, the number of individuals shedding eggs is higher from the beginning throughout the epidemic period. We also observed that for different values of the contact rate, the system still reached the endemic equilibrium. The fact that the number of infective individual, egg and larvae density increases as time progress implies that the contact rate contributes significantly to the persistence of the disease in the community. Therefore these results suggest that the pattern of soil-transmitted helminths prevalence is due to the contribution of the contact rate, which can be attributed to the poor sanitation and increased infectious larvae density in the soil. Furthermore, we can deduce that human behavioural changes that reduce contact with contaminated soil reduces transmission of the disease and slows down the egg and larva propagation speed.

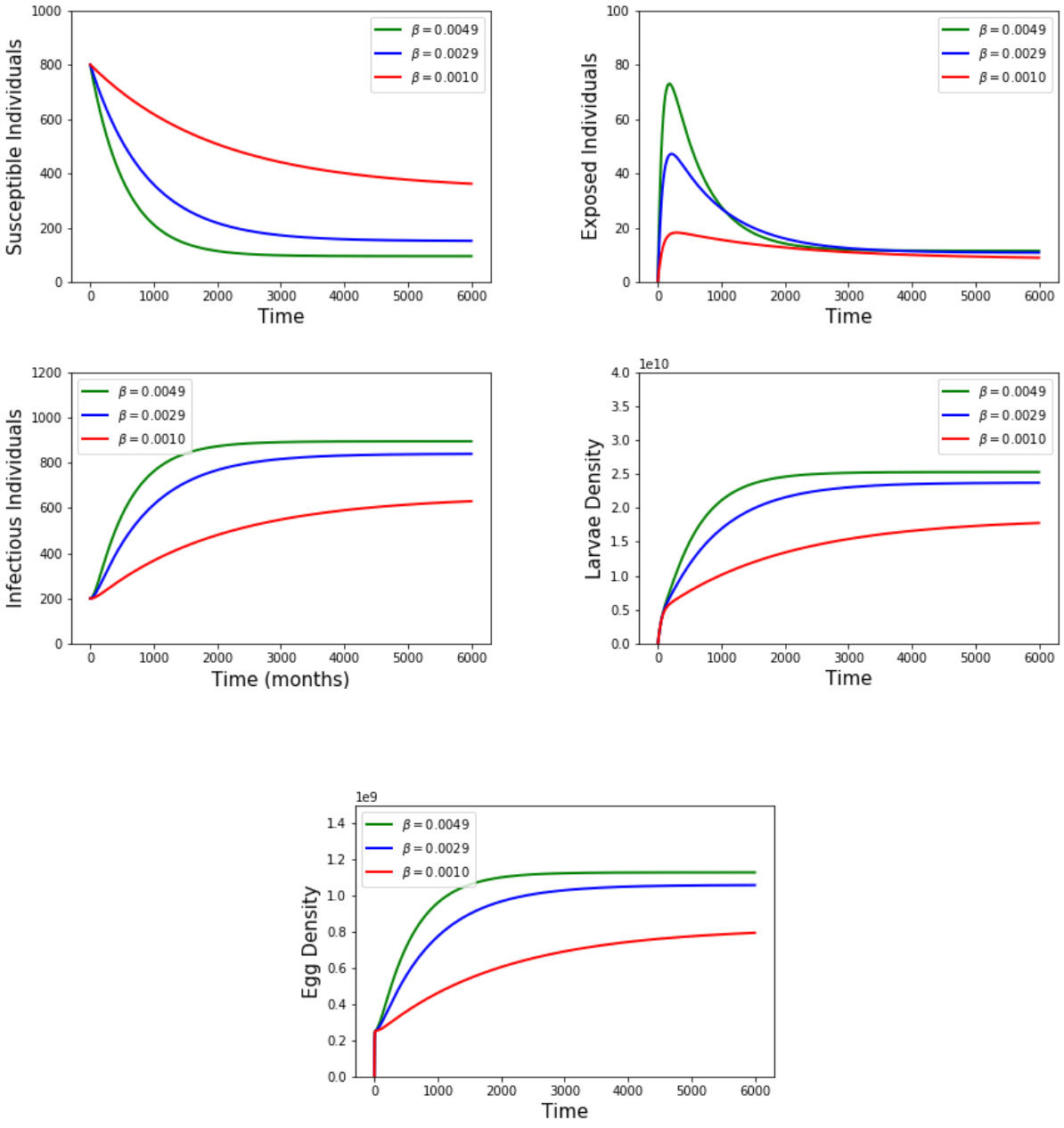

Figure 5.2 Preliminary model simulations for the soil-transmitted helminths epidemic model with varied contact rate, β.

5.5 Generalized Polynomial Chaos Model Simulation

5.5.1 Random Parameters Distribution Approximation

Transmission parameters $(\alpha, \beta, \gamma, \rho)$ are assumed to be random and follow uniform distribution, Uniform(a,b). The range for parameters in Table 5.1, used in numerical simulations was used as the support parameters for the uniform distribution. Distribution for each random parameter used in generalised polynomial chaos simulations are summarised in Table 5.3.

Parameter	Value	Source
β	Uni$(0.0265, 0.0533)$	Estimated
γ	Uni$(0.0111, 0.0167)$	[8]
ρ	Uni$(0.0200, 0.1999)$	Estimated
α	Uni$(0, 0.4)$	[8]

Table 5.3 Random parameter distribution estimation.

5.5.2 Generalised Polynomial Chaos Simulation Results

Figure 5.3, represents the population of susceptible, exposed, infectious individuals, larva and egg density in the environment simulated using the generalized polynomial chaos. The solid line represents the mean, while the grey shaded region shows the standard deviation interval for each stochastic process, i.e $\Big((S_0 \pm \sqrt{Var(S(t))}, (E_0 \pm \sqrt{Var(E(t))}, (I_0 \pm \sqrt{Var(I(t))}, (E_0 \pm \sqrt{Var(E(t))}, (O_0 \pm \sqrt{Var(O(t))}\Big)$. We observe that the polynomial chaos approach captures the output uncertainty due to randomness in the input parameters. The simulations also reveals that the population of infectious individuals and infectiousness increases to endemic equilibrium, while the population of susceptible individuals decreases.

Figure 5.3 also shows that the variance for the susceptible, exposed and the infective population slowly approaches the mean as the disease progresses to the endemic equilibrium. These results suggest the low volatility during the epidemic, and this suggests that the mean for each sub-population can be a reasonable estimate for the empirical sub-populations sizes. On the other hand, the egg and larvae density is very volatile, the variance increases as the disease approach endemic equilibrium, this may suggest that the mean does not capture the larvae and egg density appropriately.

5.6 Sensitivity analysis

We carried out the sensitivity analysis of the model using polynomial chaos-Based Sobol indices, and we did this in order to quantify the output uncertainty due to the randomness in each of the random parameters. This analysis was based on the decomposition of the variance.

Figure 5.6 - 5.8 shows the influence of parameters β, γ, ρ and α in the prediction of the model compartment sizes. We assessed the influence of random parameters on the population of susceptible individuals. Figure 5.4 shows that susceptible population is most sensitive to the contact rate β. Figure 5.5 shows that the exposed population is sensitive to the contact rate β and progression rate γ. At the beginning of the simulations, the exposed populations respond more to the contact rate and towards the end of the simulations responds more to the progression rate. Sobol's indices plots in Figure 5.6, for the effects of β in the infectious population, show that the infectious population evolution depends on the contact rate, β. Therefore, we can conclude that prevention strategy related infectious population can be an optimal policy to address the epidemic.

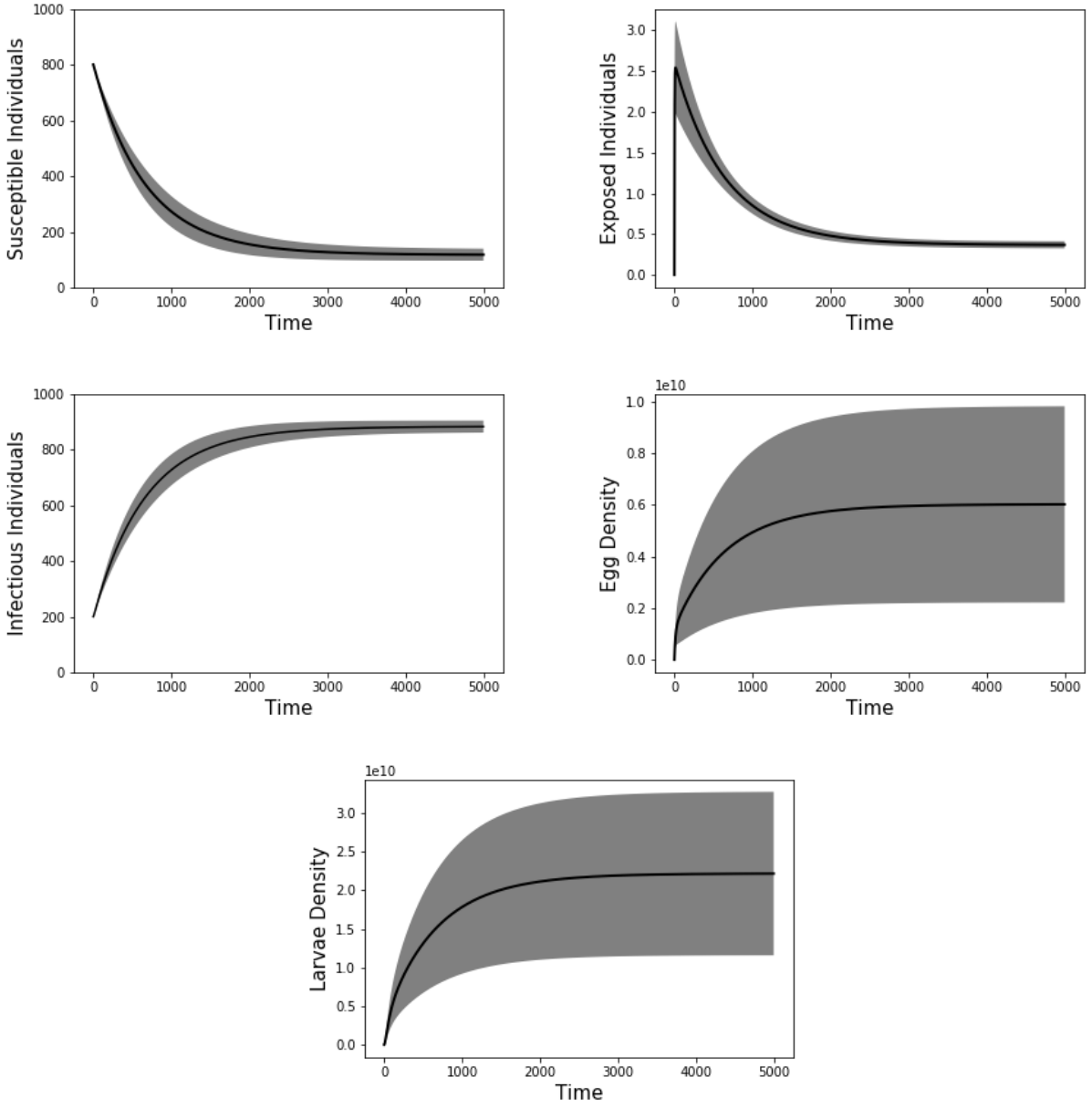

Figure 5.3 Generalized polynomial chaos method simulations. The red line represents the mean for each class in the model and the grey shaded area is the plus/minus one standard deviation from the mean for each class of the model.

Figure 5.7 and 5.8 shows that the egg and larva densities respond more on the egg shedding rate and hatching rate than other random parameters.

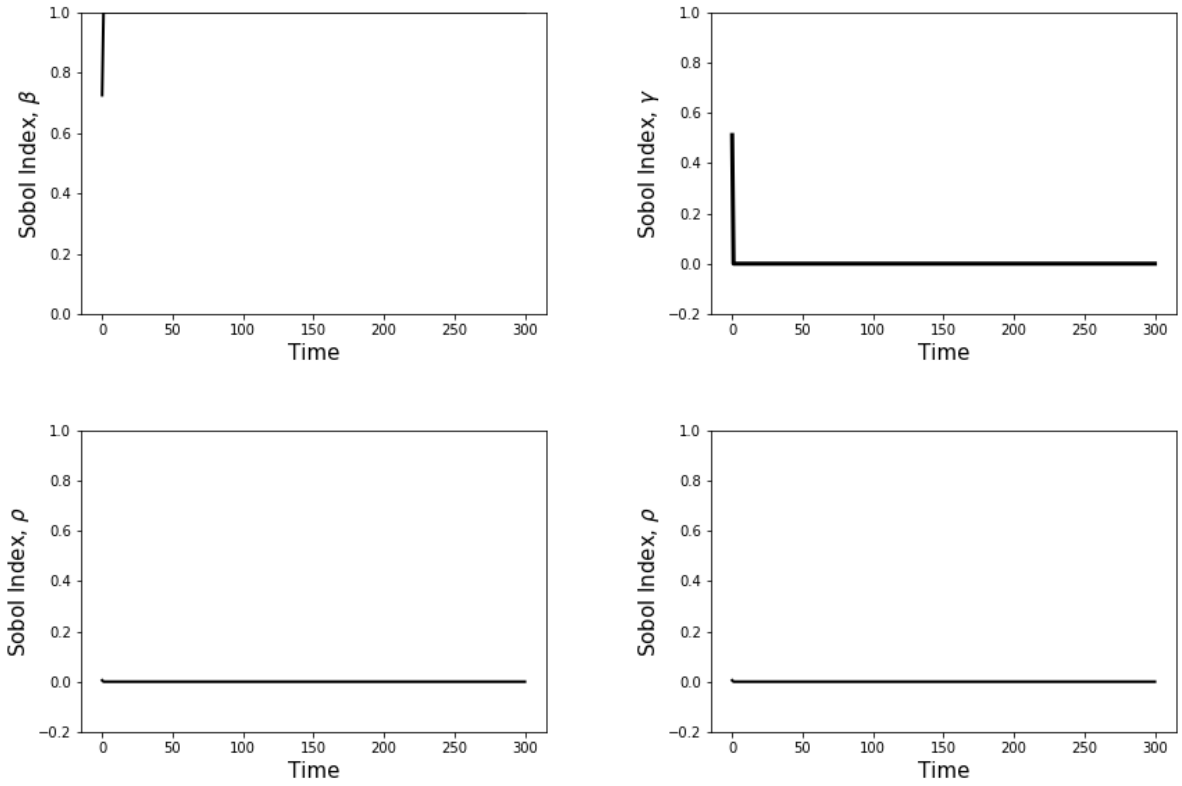

Figure 5.4 Influence of uncertain transmission parameters on the susceptible population prediction

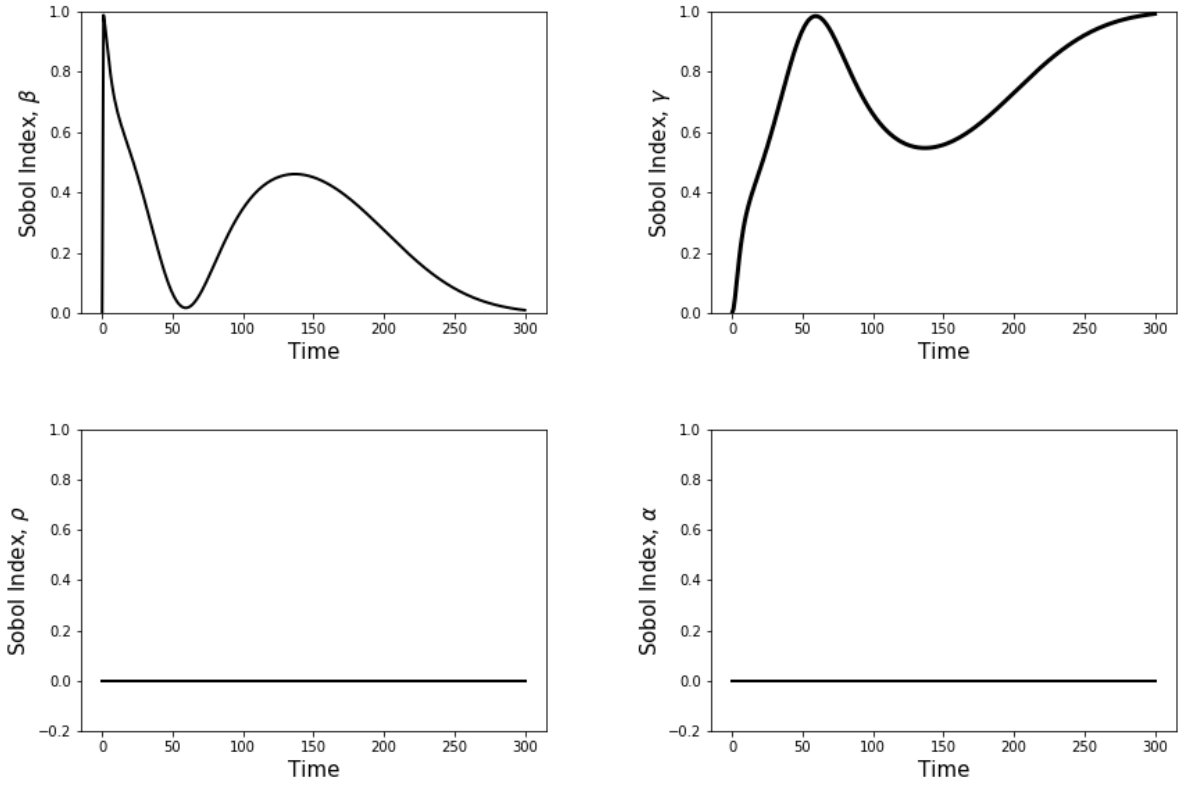

Figure 5.5 Influence of uncertain transmission parameters on the exposed population prediction

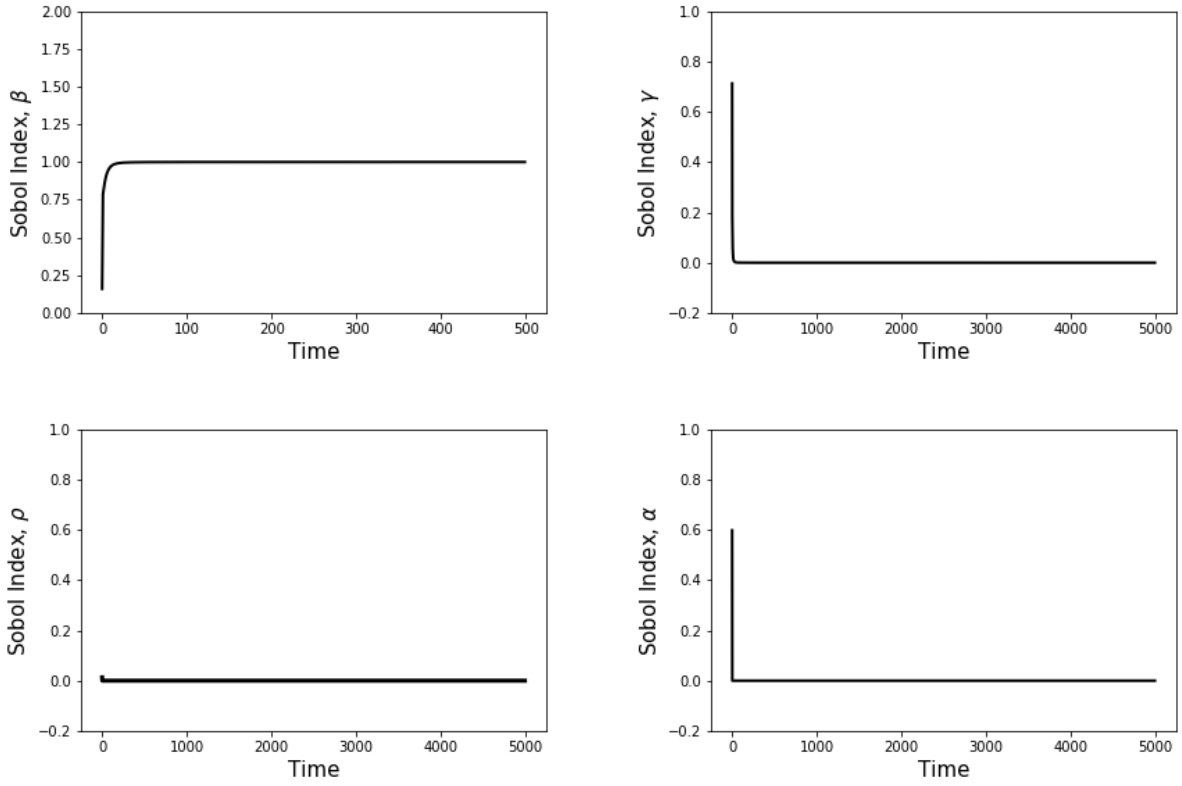

Figure 5.6 Influence of uncertain transmission parameters on infectious population prediction

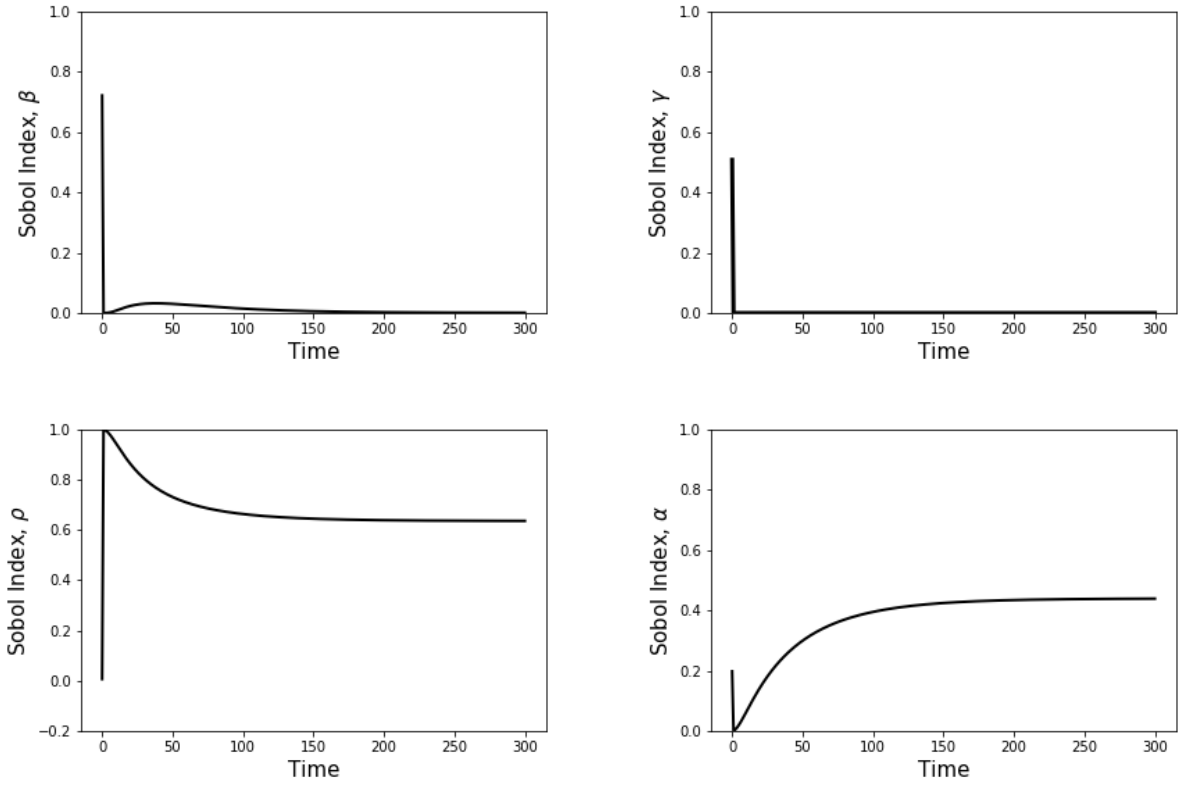

Figure 5.7 Influence of uncertain transmission parameters in the egg density prediction in the soil

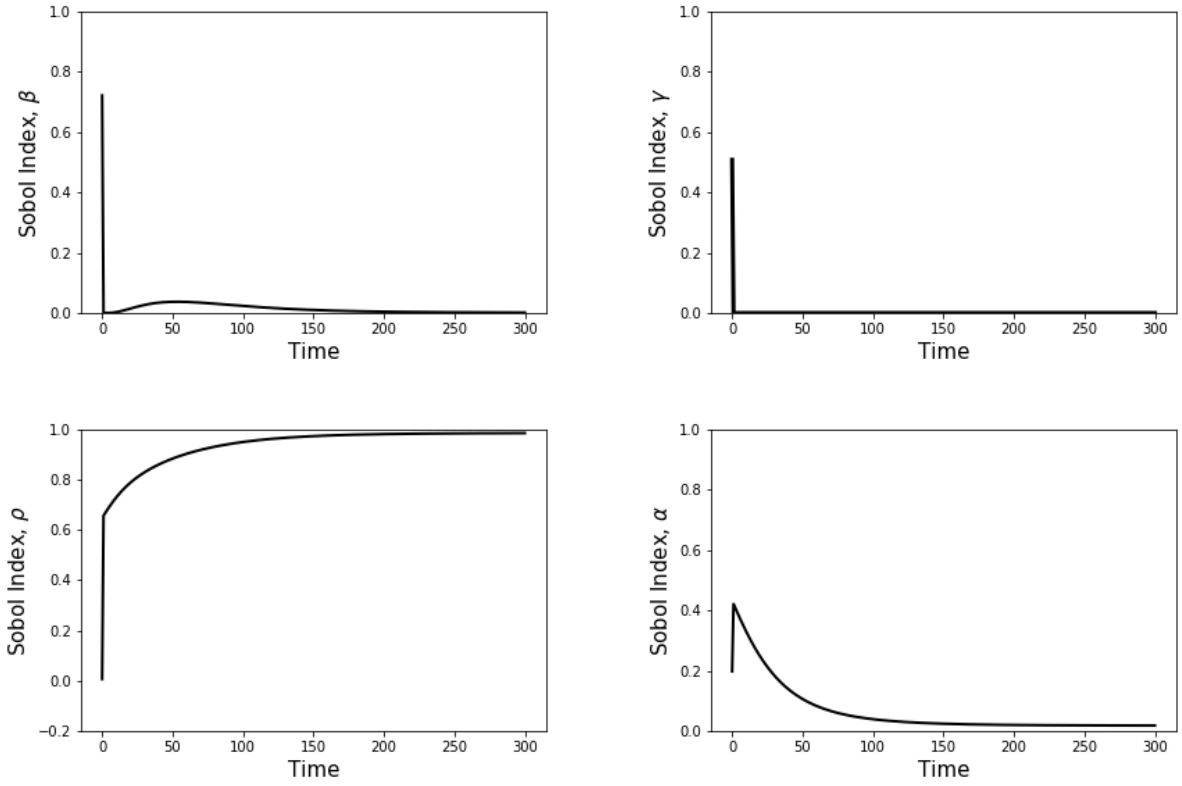

Figure 5.8 Influence of uncertain transmission parameters on the larva density prediction in the soil

5.7 Summary

This chapter presented graphical representations of the models in chapters 3 and 4. The numerical simulations were in the form of graphs. The graphs represented the predicted time series for human population interacting with contaminated soil. We presented Ascaris and hookworm numerical simulations to predict the most common STH worm infection in the human population. Furthermore, the contact rate was varied to understand the effect of human behaviour on the dynamics. Lastly, randomness in four model parameters was assumed. The generalised polynomial chaos in the numerical simulations was applied. An increase in the variance for the egg and larval density simulations was observed.

Chapter 6

Discussion And Conclusion

6.1 Discussion

In this study, we proposed a compartmental deterministic model that considers the human population interacting with soil-transmitted helminths worms in the soil. The model was designed to understand the dynamics and the effect of human behaviour on soil-transmitted helminths.

The global and local stability behaviour of the model was investigated using the Lyapunov function and the geometric method. Our analysis of the model revealed that when the basic reproduction number is smaller than a unity, the model has a globally asymptotically stable disease-free equilibrium. Furthermore, we established that there exists a unique endemic equilibrium when the basic reproduction number is more than unity and it is globally stable.

In chapter 4, we showed the possibilities of quantifying uncertainty using polynomial chaos in epidemiological models. Four transmission parameters were assumed to be functions of random variables, which changed the state variable for the model formulated in chapter 3 to be stochastic

processes. We employed the generalized polynomial chaos to incorporate the uncertainty parameter in the model. Polynomial chaos proved to be a useful method to consider the effects of randomness in the evolution of the epidemics. The method makes it easy to perform sensitivity analysis for random parameters using polynomial chaos based Sobol's indices. This study has shown how polynomial chaos can be applied in the system of ordinary differential equations to study the model more vigorously than in the deterministic approach. This method makes it possible to define the confidence interval of epidemic evolution.

Chapter 5, we investigated the effect of the contact rate in the dynamics of STH using the deterministic model developed in chapter 3. Simulations for the mean of the susceptible, exposed, infective population as well as the egg and larva density in the soil were presented. The plots also show the region one standard deviation from the mean of each stochastic process. Egg and larvae density had a more significant standard deviation as the epidemic progress compared to other state variables. Finally, we presented a sensitivity analysis for random parameters to measure the contribution of each random parameter in the variability of the infected population.

In the literature, we gathered that the hookworm species has the fastest life cycle compared to other STH species. Hence the hookworm matures faster and therefore shed egg within a short space of time compared to other species. Despite this fact, numerical simulations revealed that *ascaris lumbricoides* are the popular STH species affecting the human population, this may be caused by the number of eggs shed by one mature *ascaris lumbricoides* worm.

6.2 Conclusion

Based on our analysis, reducing the contact rate can be expected to reduce the size of the epidemic. This can be achieved by reducing the number of ways the human population interact with contaminated soil. Improving sanitation can be expected to improve most aspects of community health than reducing the soil-transmitted helminths prevalence. Greater focus is needed in putting in place safe and hygiene toilets in high soil-transmitted helminths prevalent communities.

6.3 Future work

In the future study, we could bring the model closer to reality by considering the co-existence of all three worms in human hosts. We could also explore the worm development more especially in-host worm-egg dynamics.It would be interesting to study how the amount of worms being ingested depend on the method of contamination (contaminated food, water of feaces or penetration through the skin). Our numerical analysis showed a significant value for the variance of egg and larvae density, and this suggested that the mean values simulated in generalised polynomial chaos may not be the excellent estimate of these quantities. For future work, we may look at mathematical or statistical methods to estimate these quantities or explore methods to reduce the variance so that we can estimate the epidemic with accuracy. The model can also be improved by considering intervention strategies such as vaccine and treatment. Lastly, we could estimate parameters better by obtaining more data point to obtain more accurate simulations and better approximate the distribution for random parameters.

Bibliography

[1] P. Constantine, "A primer on stochastic galerkin methods," 2007.

[2] D. S. Jones, *Differential Equations and Mathematical Biology*. Springer Netherlands, 1 ed., 1983.

[3] A. Medio and G. Gallo, *Chaotic Dynamics: Theory and Applications to Economics*. Springer Netherlands, 1 ed., 1992.

[4] R. Murray, *A Mathematical Introduction to Robotic Manipulation*. Taylor & Francis Limited, 2017.

[5] C. Castillo-ChÃąvez and B. Song, "Dynamical models of tuberculosis and their applications," vol. 1, pp. 361–404, 09 2004.

[6] "Characterizing the next-generation matrix and basic reproduction number in ecological epidemiology," *Journal of Mathematical biology*, vol. 66, no. 5, pp. 1045–1064, 2013.

[7] B. Anderson, J. Jackson, and M. Sitharam, "Descartes' rule of signs revisited," *The American Mathematical Monthly*, vol. 105, no. 5, pp. 447–451, 1998.

[8] GAHI, "Centre for disease control and prevention." https://www.cdc.gov/parasites/, Sep 2017. Accessed on 2018-01-08.

[9] GAHI, "Global atlas of helminth infection." http://www.thiswormyworld.org/maps/soil-transmitted-helminths, Dec 1988. Accessed on 2017-12-30.

[10] WHO, "World health organisation, factsheets." http://www.who.int/mediacentre/factsheets/fs366/en/#, Sept 2017. Accessed on 2018-01-07.

[11] T.-W. Jia, S. Melville, J. Utzinger, C. H. King, and X.-N. Zhou, "Soil-transmitted helminth reinfection after drug treatment: A systematic review and meta-analysis," *PLOS Neglected Tropical Diseases*, vol. 6, pp. 1–11, 05 2012.

[12] S. Brooker and E. Michael, "The potential of geographical information systems and remote sensing in the epidemiology and control of human helminth infections," in *Remote Sensing and Geographical Information Systems in Epidemiology*, vol. 47 of *Advances in Parasitology*, pp. 245 – 288, Academic Press, 2000.

[13] C. Liu, R. Luo, H. Yi, L. Zhang, S. Li, Y. Bai, A. Medina, S. Rozelle, S. Smith, G. Wang, and J. Wang, "Soil-transmitted helminths in southwestern china: A cross-sectional study of links to cognitive ability, nutrition, and school performance among children," *PLOS Neglected Tropical Diseases*, vol. 9, pp. 1–16, 06 2015.

[14] R. L. Pullan, J. L. Smith, R. Jasrasaria, and S. J. Brooker, "Global numbers of infection and disease burden of soil transmitted helminth infections in 2010," *Parasites & Vectors*, vol. 7, p. 37, Jan 2014.

[15] A. V. Fincham JE, Markus MB, "Could control of soil-transmitted helminthic infection influence the hov/aids pandemic?," 2003.

[16] E. C. Strunz, D. G. Addiss, M. E. Stocks, S. Ogden, J. Utzinger, and M. C. Freeman, "Water, sanitation, hygiene, and soil-transmitted helminth infection: A systematic review and meta-analysis," *PLOS Medicine*, vol. 11, pp. 1–38, 03 2014.

[17] R. O. M. Alaa Hammad Ali Abou-Zeid, Tigani Abdullah Abkar, "Schistosomiasis and soil-transmitted helminths among an adult population in a war affected area, southern kordofan state, sudan," 2012.

[18] I. Hagel and T. Giusti, "Ascaris lumbricoides: An overview of therapeutic targetsâĂİ, infectious disorders - drug targets," *Bentham Science Publisher*, vol. 10, no. 19, pp. 349 – 367, 2010.

[19] F. L. N. Santos, E. A. J. A. L. Cerqueira, and N. M. Soares, "Comparison of the thick smear and Kato-Katz techniques for diagnosis of intestinal helminth infections," *Revista da Sociedade Brasileira de Medicina Tropical*, vol. 38, pp. 196 – 198, 04 2005.

[20] W. H. Organisation, "Soil-transmitted helminth infections." http://www.thiswormyworld.org/maps/soil-transmitted-helminths, Feb 2018. Accessed on 2019-02-24.

[21] N. R. de Silva, S. Brooker, P. J. Hotez, A. Montresor, D. Engels, and L. Savioli, "Soil-transmitted helminth infections: updating the global picture," *Trends in Parasitology*, vol. 19, no. 12, pp. 547 – 551, 2003.

[22] M. Molvik, E. Helland, S. G. Zulu, E. Kleppa, K. Lillebo, S. G. Gundersen, J. D. Kvalsvig, M. Taylor, E. F. Kjetland, and B. J. Vennervald, "Co-infection with schistosoma haematobium and soil-transmitted helminths in rural south africa," March 2017.

[23] H. Ajoge, S. Olonitola, and D. Smith, "Soil-transmitted helminths are a serious but understudied health concern in south africa, requiring immediate attention from the scientific community. [version 1; referees: awaiting peer review]," *F1000Research*, vol. 3, no. 209, 2014.

[24] J.-M. M. Michael Baudin, "Introduction to polynomial chaos with nisp," *Bentham Science Publisher*, pp. 4 – 22, 2013.

[25] E. W. Weisstein, "Hilbert space," *MathWorld–A Wolfram Web Resource*, 2004.

[26] N. Wiener, "The homogeneous chaos," pp. 897–936, Oct 1938.

[27] D. Xiu and G. E. Karniadakis, "Modeling uncertainty in flow simulations via generalized polynomial chaos," *Journal of Computational Physics*, vol. 187, no. 1, pp. 137 – 167, 2003.

[28] D. L. Z. Robert V. Hogg, Elliot A. Tanis, *Probability and Statistical Inference*. Pearson, 2015.

[29] R. Anderson and R. May, "Helminth infections of humans: Mathematical models, population dynamics, and control," vol. 24, pp. 1–101, 02 1985.

[30] J. Truscott, T. D. Hollingsworth, and R. Anderson, "Modeling the interruption of the transmission of soil-transmitted helminths by repeated mass chemotherapy of school-age children," *PLOS Neglected Tropical Diseases*, vol. 8, pp. 1–9, 12 2014.

[31] A. Montresor, A. Deol, N. Ãă Porta, N. Lethanh, and D. Jankovic, "Markov model predicts changes in sth prevalence during control activities even with a reduced amount of baseline information," *PLOS Neglected Tropical Diseases*, vol. 10, pp. 1–15, 04 2016.

[32] B. M. Chen-Charpentier, J. C. Cortés, J. V. Romero, and M. D. Roselló, "Some recommendations for applying gpc (generalized polynomial chaos) to modeling: An analysis through the airy random differential equation," *Appl. Math. Comput.*, vol. 219, pp. 4208–4218, Jan. 2013.

[33] M. G. Roberts, "Epidemic models with uncertainty in the reproduction number," *Journal of Mathematical Biology*, vol. 66, pp. 1463–1474, Jun 2013.

[34] F. Santonja and B. Chen-Charpentier, "Uncertainty quantification in simulations of epidemics using polynomial chaos," *Computational and Mathematical Methods in Medicine*, vol. 2012, no. 6, 2012.

[35] E. H. Saturnino L. Salas, Garret J. Etgen, *Calculus one and several variables*. WilleyPlus, 10 ed., 11 2006. Pages 254 - 259 and 444 - 450.

[36] P. van den Driessche and J. Watmough, "Reproduction numbers and sub-threshold endemic equilibria for compartmental models of disease transmission," *Mathematical Biosciences*, vol. 180, no. 1, pp. 29 – 48, 2002.

[37] J. Feinberg and H. P. Langtangen, "Chaospy: An open source tool for designing methods of uncertainty quantification," *Journal of Computational Science*, vol. 11, pp. 46 – 57, 2015.

[38] S. N. Karshima, "Prevalence and distribution of soil-transmitted helminth infections in nigerian children: a systematic review and meta-analysis," *Infectious Diseases of Poverty*, vol. 7, p. 69, Jul 2018.

[39] RAJ and CO, "Hookworms in humans. symptoms. treatment. life cycle. prevention." http://rajn.co/hookworms-in-humans-symptoms-treatment-life-cycle-prevention/, Nov 2007. Accessed on 2018-09-19.